Multiobjective Mixed-Integer Bayesian Optimization for the implementation of hydrogen as maritime fuel trough Liquid Organic Hydrogen Carriers (LOHCs)

Carlos Prieto[a], Antonio Sánchez[a], Ehecatl Antonio del Rio-Chanona[b], Mariano Martín[a,*]

[a]*Department of Chemical Engineering, University of Salamanca, 37008 Salamanca, Spain*
[b]*Centre for Process Systems Engineering (CPSE), Department of Chemical Engineering, Imperial College, London, United Kingdom*

Abstract

Hydrogen is proposed as a fuel for maritime decarbonization, but its storage is challenging. Liquid Organic Hydrogen Carriers (LOHCs) offer a solution storing hydrogen under ambient conditions enabling to reuse oil infrastructure. The dehydrogenation module, coupled with a Solid Oxide Fuel Cell, is modeled using a first-principles model. Detailed three-phase reactor modeling accounts for heat, mass and momentum and represents relevant phenomena in LOHCs reactors. Two different stages are set: process design and operation. In the first one, unit design parameters and operating conditions are considered and several objectives proposed. Additionally, several reaction technologies are suggested (mixed-integer formulation). With equipment defined, operation is optimized. Expensive high-complex models hinder optimization. Hence, Machine Learning algorithms and specifically Bayesian Optimization (BO) can be leveraged for LOHCs optimization. Process design involves the optimization of a mixed-integer, single (SO) and multiobjective (MO) constrained formulation. Then, SO and MO constrained optimization are carried out for operation. To handle integers, adapted kernels and multiple acquisition function optimizers are used. These strategies perform comparably or better than approaches ignoring integers. Then, these are encouraged for an effective mixed-integer optimization. Design stage reached a trade-off with 1990 $\$/kW_{el}$ and 5.95 l/kW_{el} equipment investment and volume respectively and 37.49% efficiency. Detailed reactor models differ significantly from simplified baselines showing the need to accurately represent these units. Then, operation MO was carried out. Pareto Front was built with several operational points. Hence, the use of LOHCs for hydrogen storage in maritime sector is explored and promoted.

Keywords: LOHCs, Bayesian Optimization, hydrogen, maritime, energy storage

---

1. Introduction

The transportation sector is responsible of approximately 25% of global emissions. From them, maritime transportation represents 11% (ICCT, 2020). The International Maritime Organization (IMO) proposes a net-zero scenario for international shipping around 2050 (MEPC, 2023). The decarbonization of some activities such as refining or chemical industries is expected to be subjected to the integration between renewables and process electrification (Baldea et al., 2025). However, direct use of renewables on cargo ships is not regarded as a feasible option. Therefore, the use of low-carbon hydrogen is proposed to promote the reduction of emissions in this sector. Either fuel cells or internal combustion engines are feasible options. However, this carrier still needs to overcome the issues related to its low volumetric energy density compared to other alternatives (Hydrogen Europe, 2021). Compression and liquefaction are potential options for its storage. However, they face some challenges for its implementation on board. Compression may present safety issues and high investment whereas liquefaction has to deal with boil-off losses (Laursen et al., 2023).

Apart from traditional hydrogen storage options, other alternatives have emerged. This is the case of Liquid Organic Hydrogen Carriers (LOHCs). They can store hydrogen within their chemical structure through a catalytic hydrogenation reaction and release it in a dehydrogenation step. They provide more favorable conditions for hydrogen storage and the possibility to reuse refueling infrastructure. Several projects have appeared for LOHCs use for hydrogen storage in the maritime sector. For example, the company Hydrogenious presents a LOHCs module coupled with a fuel cell at the megawatt scale. Their project is under development for the use of benzyltoluene in maritime applications (Hydrogenious Maritime, 2023). Siemens Energy together with other partners initiated in 2021 a pilot project to evaluate the use of LOHCs in Norwegian ships (Siemens Energy, 2021). Additionally, some conceptual studies evaluated the possibilities of using LOHCs in this sector. Gambini et al. (2024a) studied hydrogen storage with LOHCs technology on a cargo ship. They analyzed the dehydrogenation process for several LOHCs under dynamic conditions. It was concluded that hydrogen production can be effectively modified according to ship power demand. They proposed the use of Solid Oxide Fuel Cell (SOFC) to cover the LOHCs dehydrogenation heat. However, they did not study heat integration from the process perspective. Therefore, detailed process analysis is required to explore the opportunities of this integration in the maritime sector.

*Corresponding author
Email address: mariano.m3@usal.es (Mariano Martín)

Here, a conceptual process optimization is proposed for the implementation of LOHCs to be used in ships for hydrogen storage. To the best of the authors' knowledge, a detailed flowsheet is never proposed and optimized for LOHCs used for maritime applications. The process is composed of a dehydrogenation (DH) module using dibenzyltoluene. It is coupled with a Solid Oxide Fuel Cell (SOFC). It can provide the power for the ship and heat for LOHCs dehydrogenation. It acts as a Combined and Heat and Power (CHP) module. A holistic approach is used for detailed process assessment. As in other works, investment minimization is accounted for. However, other areas such as fuel use efficiency, risk minimization or equipment volume (critical for maritime applications) are also taken into account.

Two stages are considered for LOHCs optimization. First, a process design stage is introduced. Optimization for process operating conditions (e.g., reaction pressure and temperature, the recycle ratio) and design parameters (e.g., reactor dimensions) needs to be done to meet ship energy demand (process constraints). Additionally, in the design stage, different reactor technologies are proposed to be used in the dehydrogenation section (isothermal and adiabatic). To perform reaction technology selection and determine the number of units for each type, integers must be introduced in the formulation. The modeling of reaction units has been addressed in several studies, employing different levels of complexity. Some approaches represent reactor performance using intrinsic kinetics and equilibrium calculations as shown in Gambini et al. (2022), who indicated that such formulations could serve as a basis for more detailed models using ordinary differential equations. Heublein et al. (2020) demonstrated that different reactor configurations can lead to markedly different hydrogen yields, with reference to phenomena such as potential catalyst dewetting. These findings indicate that LOHCs reaction progress cannot be described by kinetics alone, but also requires explicit consideration of reactor design and hydrodynamics. In addition, equilibrium-based calculations were shown to significantly overestimate hydrogen yield compared to actual reactor performance under different conditions. In previous work, mass, heat and momentum transfer have been accounted for different reactor designs (Prieto et al., 2023). The developed model included external and internal mass transfer, heat transfer between bulk liquid and particle and heating media as well as hydrodynamics. In the case of fixed-bed reactors, liquid holdup (static and dynamic), pressure drop and catalyst wetting efficiency are explicitly considered, as these are critical for reactor design and scale-up. Other modeling approaches in the literature capture some of these aspects but still neglect key transport phenomena. For example, Geißelbrecht et al. (2024) modeled the performance of a cuboid reactor including intrinsic kinetics, equilibrium and relevant vapor-liquid equilibrium, but did not account for mass transfer limitations, pressure drop or catalyst wetting. Rao et al. (2022) incorporated mass transfer effects. However, liquid evaporation or pressure drop were not considered. Gambini et al. (2024b) reflected the importance of operating above atmospheric conditions to overcome pressure drop, but did not explicitly define mass transfer, liquid holdup or evaporation phenomena.

Overall, while existing models have made efforts to represent this system, some critical aspects are often omitted. Therefore, in this work, and based on previous one, several reactor modeling elements are identified as essential. These are systematically combined within a first-principles framework (Prieto et al., 2023). This refined model accounts for mass, heat and momentum transfer, vapor-liquid equilibrium and extends the original adiabatic fixed-bed formulation to represent multitubular isothermal reactor configuration. However, the combination of integers with the high complexity of these models (non-linearities and differential equations) and the interaction with other process units, makes it challenging to perform optimization with gradient-based approaches. Additionally, each model evaluation is expensive. The second stage is referred to as process operation. After providing equipment sizing (number and type of reactors, dimensions, heat exchange areas), operation can be optimized under stationary conditions for various energy demands. This is to mimic different operational points during ship journey. The different operational states analyzed reflect the range of situations in which the ship could operate based on proposed LOHCs system. These have been treated as stationary based on previous work demonstrating the fast dynamic response of this technology, in the order of minutes (Gambini et al., 2024a). For this second stage, operating conditions are optimized based on the ship energy requirements. Similar limitations are found in process operation optimization compared to previous process design stage (high complexity of models and expensive functions). However, in this case, since reactors are already set, no integer decisions are present in the formulation.

At this point, Machine Learning (ML) techniques, specifically data-driven methods, can help to deal with costly process simulations (van de Berg et al., 2022). For instance, Bayesian Optimization (BO) is a data-driven technique used to optimize black-box function problems. It is based on the optimization of a surrogate model, typically a Gaussian Process (GP). The GP is trained from the input variables and results from the objective function. An acquisition function is used for the selection of the most promising candidates to be evaluated next, and these new datapoints are incorporated to the GP model. This procedure is done iteratively (Garnett, 2023).

Alternative optimization strategies can also be considered for process design. Overall, other possibilities to handle optimization include deterministic and stochastic gradient-based algorithms, metaheuristic methods, and Design of Experiments (DOE)-based surrogate approaches. Deterministic gradient-based algorithms are efficient in smooth continuous domains, but their performance degrades sharply in the presence of discontinuities or non-differentiable transitions typically introduced by integer variables (Gómez-Castro and Rico-Ramírez, 2025). Stochastic or approximate gradient methods suffer from similar limitations and often become unreliable when gradients are noisy, undefined, or prohibitively expensive to evaluate. Metaheuristic strategies such as Genetic Algorithms, Particle Swarm Optimization or Simulated Annealing can handle mixed-integer search spaces, but they typically require a large number of evaluations to converge, which is impractical for expensive simulations or experiments (Ong and Teo, 2021; Wu et al., 2024). Benchmark studies comparing gradient-based approaches against Bayesian Optimization (BO) have shown that BO consistently converges to superior solutions (Zhao et al., 2025). Apart from solution quality, computational cost is a key differentiating factor. For gradient-based approaches, when analytical gradients are unavailable, numerical gradient estimation requires at least one additional function evaluation per decision variable and per iteration, leading to a computational cost that scales linearly with the problem dimension (Nocedal and Wright, 2006). Consequently, even for a moderate number of design variables, the total number of function calls rapidly exceeds that of BO. This effect has been reflected in Diessner et al. (2024) where a gradient-based optimizer required at least six times more objective function evaluations than BO in a continuous optimization problem. An even larger gap is expected in mixed-integer formulations, where gradient information is either unavailable or unreliable, making such computational overhead unacceptable when objective evaluations are expensive. These differences are further amplified for metaheuristic methods. Although in some cases minimum computational budgets of approximately 250 iterations are reported, these values already exceed typical BO budgets for expensive optimization problems. More generally, recommendations of 50 iterations per decision variable are common, and significantly larger budgets are often required to avoid premature stagnation and ensure convergence, with improvements sometimes observed only after hundreds of thousands of iterations (Kazikova et al., 2021). Surrogate-based optimization from a fixed DOE is another possible alternative, but relying on a static global model often fails to focus sampling on the regions where optimal values are located. Hence, a higher number of iterations is expected to this alternative compared to BO to reach comparable results. Overall, mixed-integer expensive optimization remains challenging for traditional methods, which generally require an excessive number of iterations and thus become infeasible for high-cost objective functions (Zhang et al., 2020). BO is able to perform optimization within a reduced number of iterations. Another advantage is that the objective function is directly evaluated from the real function. This is particularly useful in formulations including, for instance, differential equations. Otherwise, alternative approaches need to be used (e.g., discretization, surrogate models). Therefore, the use of BO is highly encouraged for LOHCs process optimization, considering the presence of rigorous reactor modeling in the formulation. BO has been already proposed for the optimization of complex process scale formulations (Paulson and Tsay, 2025). For instance, it has been applied for some applications such as ethylene oxide optimization using design and operating parameters (Iwama and Kaneko, 2021). Similar process design examples using BO include the optimization of CO_2 adsorption or DME production (Ward and Pini, 2022; Nakayama and Kaneko, 2023). And, specifically, this ML technique has also been applied in the LOHCs field for dehydrogenation reactor optimization as an isolate unit by Verhoolen et al. (2024). Hydrogen production was set while operating conditions such as temperature are minimized and final conversion maximized. However, apart from reactor optimization, the entire process design needs to be addressed and other areas analyzed (e.g., energy efficiency, safety, volume).

At the same time, BO can be adapted based on the requirements of the LOHCs process optimization problem. For example, while this framework can be applied to single objective optimization, the possibility to account for several objectives at once, as done in this work, and perform multiobjective optimization (Fromer et al., 2024) has also been considered. Other interesting features that BO offers are the option of evaluating feasible points (constrained BO) (Amini et al., 2024), or handling integer or categorical variables (mixed integer). For mixed-integer optimization, some variable transformations may be done as formulated in Bartoli et al. (2025). Other strategies are proposed to handle the presence of integers. For example, Morlet-Espinosa and Flores-Tlacuahuac (2024) evaluated the use of different surrogates (GPs, Sparse GPs or Student-T process) and the combination of continuous and integer kernels. Garrido-Merchán and Hernández-Lobato (2020) performed a comparison between several alternatives using the Spearmint library. They introduced approaches which rounded integer variables either before evaluation or inside the function wrapper. However, the most effective approach in that study accounted for the presence of integer variables by modifying the kernel. It led to improved performance when the kernel was adapted to reflect the discontinuity introduced by integers.

The popular Python library BoTorch includes a wide range of options to perform BO. For example, among other possibilities, constrained BO or multiobjective optimization can be implemented. In the presence of integer variables, BoTorch framework also offers optimizers designed for mixed-integer spaces. However, to the best of the authors knowledge, the GPs used to model objectives and constraints can only be adapted to such spaces when variables are categorical, using the Hamming distance (Balandat et al., 2020). In contrast, discrete spaces with ordinal variables are treated as continuous, meaning that integer discontinuities are not captured by the GPs. At this point, a comparison should be made between this approach and others that account for such discontinuities to identify opportunities for BO to handle integers.

In this work, first, the optimization of DH and CHP modules process design and second, the optimization of process operation once equipment design is set, are performed. For that purpose, BO is used. In the process design stage, single and multiobjective optimization of a complex, mixed-integer, constrained process system for hydrogen use in the maritime transport sector is performed. Given the presence of integer variables in the formulation and the necessity to account for them, a comparison is provided between different strategies integers may be handled. For instance, the use of a standard RBF kernel is compared with a modified kernel that incorporates the transformation proposed in Garrido-Merchán and Hernández-Lobato (2020) to handle integer discontinuities. Additionally, several optimizers are employed for the acquisition function optimization in the mixed-integer space. Afterwards, single and multiobjective constrained BO are performed for process operation optimization. The rest of the paper is structured as follows: Section 2 introduces the methodology, Section 3 presents the results for the different case studies and finally Section 4 draws up some conclusions.

2. Methodology

In this work, BO is applied for the optimization of LOHCs DH and CHP modules. Hydrogen is used in a fuel cell to run the different engines of the ship and provide for the heat for endothermal dehydrogenation. The system to be optimized, considers a rated power of 12 MW (main and auxiliary engines) (Gambini et al., 2024a).

First, in this section, the LOHCs DH and CHP modules description and modeling are introduced. Then, two well differentiated stages are defined: process design and operation. First one consists of a process superstructure optimization (reaction technology selection) and the sizing of the main process equipment. A multiobjective problem is formulated to balance key performance indicators, which are sometimes conflicting. For instance, it is reasonable to expect lower risks when less demanding conditions are used in the process. Nevertheless, this may negatively influence the sizing and investment of related process equipment. Additionally, LOHCs fuel efficiency, directly related to LOHCs conversion, may result in a worst catalyst use to reach higher dehydrogenation degree. This may translate into a higher economic burden and bigger equipment.

Dehydrogenation reactors selection and process operating and design parameters are introduced as input variables. Finally, ship energy demand is established as a constraint. After the main process equipment is sized, process operation is optimized considering the design from the previous stage. Stationary conditions are considered since the operation for hydrogen-fueled ship journey using LOHCs technology occurs mostly in the steady state (Gambini et al., 2024a). Since different energy demands are expected during a journey, several operation scenarios (25%, 50%, 75% and 100% engine use) are imposed as constraints and optimized. In this case, single and multiobjective constrained optimization is carried out only considering process operating conditions.

The techniques and elements used for BO are also introduced in this section (e.g., acquisition function, GPs, single/multiobjective optimization). Additionally, in the case that integers are present in the formulations, different approaches are presented and tested to handle integer variables (kernel and optimizers). Hence, the methodology section includes DH and CHP process description and modeling, description of the two stages of the optimization (process design and operation) and BO algorithm used.

2.1. Process model

The hydrogenated LOHCs may be loaded to the ship instead of conventional maritime fuel. Then, a dehydrogenation module inside the ship releases hydrogen to fuel the ship. For this purpose, dibenzyltoluene appears as a promising candidate. This molecule presents attractive features for this purpose. It has high storage capacity, is considered as a safe compound (low toxicity and flammability), presents low volatility and melting point and it is a cheap and extended chemical worldwide (Niermann et al., 2019; Abdin et al., 2021; Prieto et al., 2025). Indeed, dibenzyltoluene has been proposed in other works where LOHCs were proposed for maritime transport (Gambini et al., 2024a). Then, the hydrogen released is fed in a fuel cell. It can operate as a CHP system. Electricity is used to cover the demand for the engines and other units in the process. The heat can be recovered to meet the LOHCs dehydrogenation energy. If required, additional hydrogen is burnt. The DH and CHP modules description and modeling are presented in the following subsections.

2.1.1. Dehydrogenation and CHP modules description

In this section, a process superstructure for the dehydrogenation module is described. Different reaction technologies are proposed to perform LOHCs dehydrogenation: multitubular isothermal and adiabatic reactors. A general flowsheet is depicted in Figure 1.

Perhydro-dibenzyltoluene has been conveniently produced onshore by an external supplier. To meet the engine power demand, this LOHC is fed to dehydrogenation mod-

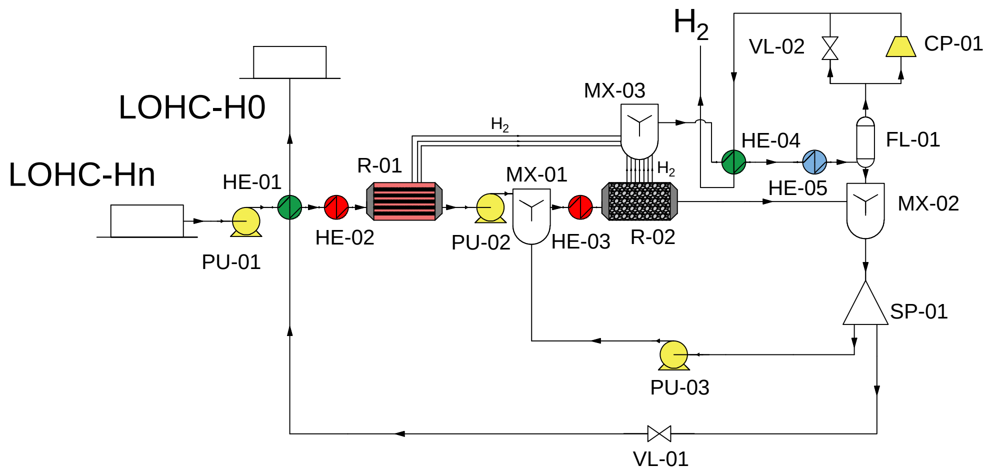

Figure 1: Dehydrogenation module for hydrogen release in cargo ships with two potential reaction technologies.

ule to release hydrogen. This reaction needs to consider several areas together: heat transfer, thermal energy management, reactor volume minimization, pressure drop, LOHCs evaporation minimization and an efficient use of precious metal catalyst (Prieto et al., 2023; Willer et al., 2024a,b; Kadar et al., 2024). The dehydrogenation module proposed in this work is composed of several reaction technologies. These include isothermal (R-01) and adiabatic (R-02) trickle bed reactors. First, a pump (PU-01) is used to increase the pressure of the liquid to the reaction conditions of the isothermal reactors. Then, a heat exchanger (HE-01) is used to recover energy from the hot LOHCs products coming from dehydrogenation. A second heat exchanger (HE-02) adjusts the temperature of the stream to the dehydrogenation conditions before it is fed to the reaction units. A detailed scheme of the reaction section is shown in Figure 2.

Several isothermal and adiabatic reactors may be placed in a series configuration. This alternative is explored because of ship dimension limitations. In some cases, having a single unit may not be enough to release the required amount of hydrogen. Reactor units must fit within the ship maximum height. At the same time, including several units may enhance LOHCs performance (e.g., lower pressure drop and evaporation). The isothermal reactors are expected to reach higher conversions at the beginning of the reaction. This is because better temperature control provides more efficient catalyst use. It makes sense to exploit this feature and locate these units first. However, adiabatic

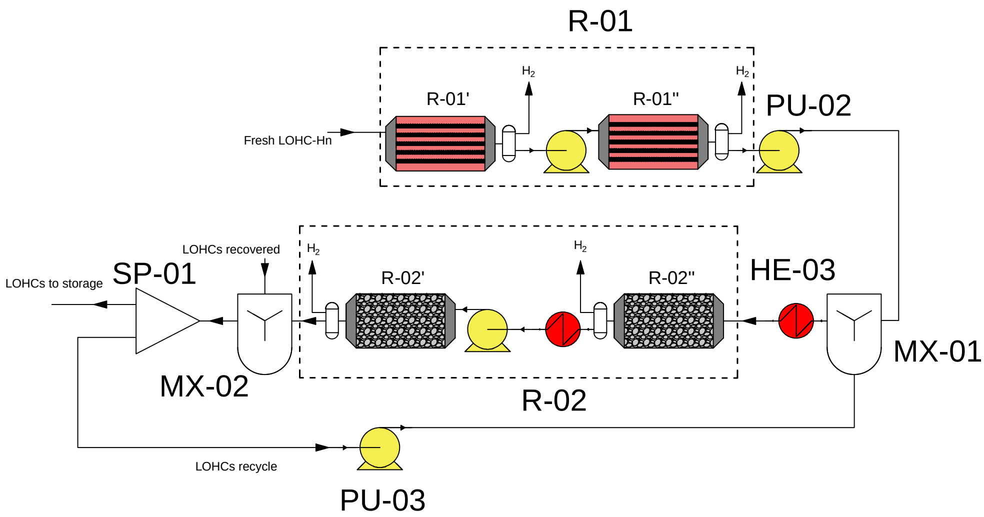

Figure 2: Detailed dehydrogenation section with isothermal and adiabatic reactors for hydrogen release and secondary equipment (heat exchange and pumping equipment).

units can be regarded as interesting options to be used above certain degree of dehydrogenation. Low reactant concentrations can reduce the impact of the temperature reduction from the adiabatic mode (Prieto et al., 2023). Then, it can outperform heated-multitubular reactors in terms of lower LOHCs evaporation. This aspect is critical for energy efficiency. Additionally, lower reactor volumes or easier operation is expected. Hence, a first set of isothermal reactors is proposed followed by a series of adiabatic beds. After each isothermal and adiabatic reactor, the gaseous phase is separated. This is to avoid larger LOHCs evaporation and pressure drops. Then, the liquid phase is set again to the operation pressure with intermediate pumps. This procedure is done successively between all the reaction units. After the last isothermal reactor, the liquid product is directed to a second section where adiabatic reactors are installed. Previously, the LOHCs can be mixed with a recycle stream (MX-01). The use of this recycle is proposed to minimize the temperature drop along the different adiabatic reactors. Likewise for the isothermal units, the pressure is adjusted with intermediate pumps. However, in this case, intermediate heat exchangers are also used to reheat the liquid to the operating conditions between stages.

After the reaction section, the dehydrogenated LOHCs are then either recycled back to the adiabatic reactors to increase LOHCs conversion or stored. Previous to the storage, the high temperature of the stream is used to preheat (HE-01) the fresh raw material. With regards to the gaseous phases from all the reactors, these are all mixed

(MX-03) and cooled. This is done to recover the LOHCs species present in the gaseous phase due to evaporation. The cooling of these gaseous streams is performed in two stages. The first one reheats the final hydrogen product integrating heat (HE-04) and thus, improving CHP module efficiency. Then, an air-cooled heat exchanger (HE-05) is used to further reduce the temperature to 313 K (Preuster et al., 2018). Hence, hydrogen product stream removes the LOHCs impurities and is reheated in HE-04.

The final hydrogen product is used to produce power. This serves to run the main and auxiliar engines of the ship and some units of the process (pumps, air blowers and air coolers). Fuel cells have been proposed as a potential conversion technology. Among the possibilities, Solid Oxide Fuel Cells (SOFC) are highly encouraged in the context of LOHCs utilization. The high operating temperatures of this device can be considered to supply LOHCs dehydrogenation energy (Preuster et al., 2018; Distel et al., 2025). The use of heating oil to heat dehydrogenation reactors has been proposed in the physical implementation shown in Eypasch et al. (2017). There, natural gas is burnt to raise its temperature. Similarly, the hot gases from the SOFC can be used to heat a heating oil. This hot oil provides a more uniform temperature difference in the reactors compared to hot gases. At the same time, lower temperatures are also provided to improve reactors and heat exchangers material durability. Hence, thermal oil is used in isothermal reactors and other heat exchangers from the dehydrogenation module. Furthermore, the hot gases from the SOFC are used to preheat hydrogen and air to the operating conditions of the SOFC. With this idea, the CHP proposed in this work is shown in the Figure 3.

The hydrogen from the dehydrogenation module is either compressed (CP-01) or expanded (VL-02). It depends on the final operating conditions of this module. Then, it is preheated in HE-06 with SOFC anode exhaust gas. Similarly, air in excess is compressed (CP-02) and preheated (HE-07 and HE-08). The electrochemical reaction is performed in the fuel cell (FC-01). The gases inlet and outlet temperatures are set to 873 K and 1073 K respectively. The pressure drop is accounted for to estimate the air blower demand (Peters et al., 2016). Two output streams exit from the fuel cell, one from the anode and another from the cathode. These are mixed to burn the unreacted hydrogen (B-01). The heat from this stream is used for the reheat of the oil to be used in the process (HE-09) and for air stream preheating (HE-07 and HE-08) before the fuel cell. If additional energy is required, part of hydrogen is directed to the burner instead of to the fuel cell.

2.1.2. Dehydrogenation and CHP modules modeling considerations

To model both DH and CHP modules, some assumptions are made for each process equipment. These are described in the following for each one:

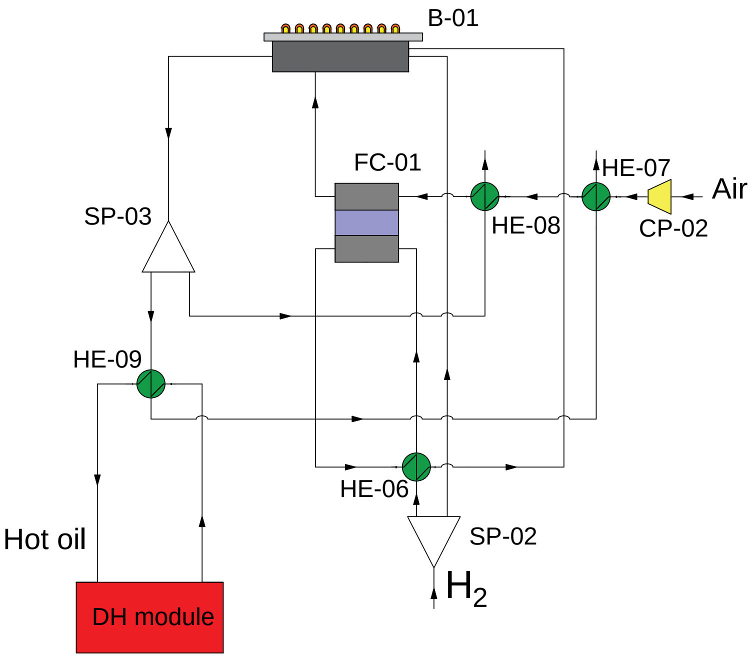

Figure 3: CHP module with SOFC technology for power production to run ship engines and heat used in DH module.

1. Dehydrogenation reactors: Adiabatic and multitubular isothermal trickle bed reactors are considered as potential technologies for dehydrogenation. The modeling of the adiabatic reactors is based on previous work (Prieto et al., 2023). In the case of isothermal units, also trickle bed reactors, the previous model can be adapted with some modifications and assumptions detailed in the Supporting Information.
2. Heat exchangers: To perform the energy balances, some differences exist between the design and operation of the process. For process design, the heat exchange area is not established yet. Hence, either a final process temperature (reactors, fuel cell, separation inlet temperatures) or a 5 K temperature approach is considered (heat exchangers with integration between streams and air coolers). Differently, for the process operation, the area is already set. Then, either the amount of utilities (hot oil, air flow) or the final temperatures are adjusted based on the available area. Moreover, in the case of air coolers, there is a blower. The energy demand is calculated based on typical pressure drop (Sinnott and Towler, 2020).
3. Flash separators: Liquid-vapor equilibria of the LOHCs compounds is considered

for these units based on its vapor pressures (Müller et al., 2015).

4. Pumps and compressors: To calculate the power demand for air blowers, air is assumed to behave as an ideal diatomic gas ($k_p = 1.4$) and 75% isentropic efficiency is applied. With regards to the pumps, these are assumed to have a 75% efficiency (Couper, 2005).
5. Fuel cell: 85% fuel utilization is set as the operating point for the fuel cell. Typical fuel cell parameters are considered from Peters et al. (2016) and electrical yield is calculated according to the equations presented on the same work. Additionally, 95% AC-DC converter efficiency is set.

2.2. LOHCs Optimization: Process design and operation

Two different modes are considered for DH and CHP modules optimization: process design and operation. The first one involves the design and purchase of the process equipment (e.g., reactors, heat exchangers, fuel cell). Based on the results from this stage, process equipment dimensions are set (e.g., reactor catalyst and diameter, heat exchange areas).

The LOHCs technology has been simulated under dynamic conditions in Gambini et al. (2024a) to run a ship during a typical journey. Minimal misalignment was found between hydrogen supply and demand. The dynamic response of LOHCs was able to adapt to hydrogen demand within few minutes. This represented a minor contribution to the total duration of the journey. In comparison, several stationary states with several hours of duration were revealed over the journey. For the step transitions, the delay time and overshoot present low intensity and short duration with minimal misalignment while during ramp transitions, the misalignments are further reduced. Therefore, it is reasonable to expect that LOHCs systems may operate most of the time in stationary state conditions around several operational setpoints. Hence, steady-state simulations for several nominal cargo ship loads may be considered to be representative for the operation of these LOHCs systems in cargo ships. Then, based on already set process equipment, the operation of this process under stationary state conditions is considered. It is optimized for several energy demands. The long-term operation of cargo ships may be affected by additional uncertainties such as LOHCs degradation, catalyst ageing, equipment fouling, or maintenance requirements. In practice, many of these issues can be addressed during scheduled maintenance periods in port, similar to the routine procedures commonly applied in chemical processing plants operating with comparable catalytic and thermal equipment. However, the quantitative assessment of these effects would require extensive long-duration experimental data, which is currently limited, and therefore lies outside the scope of this work.

First, for the design stage, constrained mixed-integer single objective optimization is performed for each objective function presented in the following (equipment investment and volume, fuel efficiency and risk). The constraints are based on the energy demand to meet (at least 12 MW). The number of reaction units introduces integers in the formulation. Next, constrained mixed-integer multiobjective optimization is proposed to reach a trade-off between objectives. To select a final process design among the feasible candidates, a quantitative Multi-Criteria Decision Making (MCDM) method is employed. In this work, the Utopia Point method is adopted. The Utopia Point represents an ideal solution in which the optimal value of each conflicting objective function is simultaneously achieved. Accordingly, the Utopia Point is defined using the optimal results obtained from the corresponding single-objective optimizations. The non-dominated solutions obtained from the multiobjective optimization define the Pareto Front and are compared with the Utopia Point. For each Pareto solution, the Euclidean distance to the Utopia Point is computed, and the solution exhibiting the minimum Euclidean distance is selected (Szparaga et al., 2019).

After that, the operation mode is optimized. In this case, design parameters are fixed from the previous stage. Then, no integers are present in the formulation and the problem becomes a continuous-space optimization problem. Constraints are adjusted to the different energy requirements. However, in this case, the objectives directly related to process equipment (investment and volume optimization) are not considered. This is because the process is already set and optimization of these functions no longer makes sense. Then, only objective functions that can be modified by operating conditions (fuel use efficiency and risk minimization) are accounted for in this analysis. Hence, single and multiobjective constrained optimization are performed for operation mode.

Note that system is optimized using a sequential two-stage approach. First, power system process design is optimized and set. Then, operation is optimized for various energy loads. It is recognized that the possibility to optimize this energy system considering simultaneously process design and operation would be a suitable approach. However, note that for this specific application, it is not possible to determine a representative ship power load profile that is valid for all situations. This is due to the singularities associated with each individual voyage. Therefore, the selection of a specific mission is considered to be out of the scope of this work. Overall, ships, and transport applications in general, are typically designed for a standard rated capacity. The complexity of powertrain systems promotes the use of standard rated power provided by equipment suppliers. Consequently, the same ship nominal power design is employed across different voyages with very different characteristics (e.g., duration, weather conditions, cargo, distance). Since it is not useful to determine a specific power profile, power system is designed for the worst-case scenario (e.g., 12 MW nominal power) which may be required under adverse weather conditions. At the same time, as demonstrated in the Results section, the final results do not differ significantly between nominal capacity and reduced process loads. Hence, it can be demonstrated that the results for nominal capacity have a great influence on the other operational loads.

2.3. *Objective functions*

To favor the use of LOHCs for maritime applications, several dimensions must be assessed and optimized. Therefore, in this work, a multiobjective optimization approach is proposed.

2.3.1. *Investment cost*

The economy of the sector depends on the investment cost of the ship and related equipment. The scope of this work is limited only to the optimization of the LOHCs dehydrogenation and use of hydrogen in the fuel cell. The equipment included in the calculations corresponds to the heat exchangers, pumps, fuel cell, air blowers, air coolers (including its respective air blower) and reactors. The investment for other equipment such as flash vessels, mixers or splitters is assumed to be negligible.

At the same time, it is important to include fuel utilization in this objective but without imposing significant priority on fuel use. Otherwise, either process equipment would be oversized or LOHCs may be used inefficiently. In other processes, it is common to compute the total investment of equipment, for example reactors, but also account for the degradation/losses of catalyst or closed loop refrigerants. Likewise, LOHCs losses are expected to be present on this system. Therefore, we include in this objective a penalty to replace LOHCs losses to favor efficient fuel use. To compute the economic cost of LOHCs degradation, a 20-year period is assumed to make LOHCs losses comparable with equipment investment. To estimate the cost to replace the LOHCs lost in the process, 0.1% losses per cycle and an average purchase cost of 4 \$/kg are taken (Niermann et al., 2019). An average ship utilization of 4320 h per year is assumed (Korberg et al., 2021). Note also, that the nominal power installed on a ship is not required in most cases. It is only demanded under adverse weather conditions. Therefore, a conservative 65% average utilization of the ship engine capacity is used to perform the calculations (Gambini et al., 2024a).

Hence, this objective function will be composed of the equipment investment cost (EIC) and materials replacement cost (LOHCs losses) (MRC) as shown in Eq. 1.

$$\mathrm{f}_1 = \mathrm{EIC} + \mathrm{MRC} \tag{1}$$

2.3.2. *Hydrogen to energy efficiency*

The feasibility of LOHCs to promote the utilization of hydrogen as fuel is directly related to the system efficiency and conversion degree. These need to be maximized to reduce fuel use, which directly impacts on the operating costs of the ship but also on the volume of fuel stored on the ship. The hydrogen released during dehydrogenation can be used in the fuel cell to produce electricity or burnt. Hence, the Eq. 2 is proposed to maximize fuel energy use of the hydrogen stored with LOHCs technology. There, DoDH represents the degree of dehydrogenation, $F_{H_2,released}$ the hydrogen released in the dehydrogenation module and E_{H_2} the energy available in the hydrogen released.

$$f_2 = 100 \cdot \mathrm{DoDH} \cdot \left(\frac{\mathrm{NP}}{F_{H_2,released} \cdot E_{H_2}} \right) \tag{2}$$

To obtain the net power produced (NP), Eq. 3 is introduced, where W represents the power produced/consumed on each process unit.

$$\mathrm{NP} = W_{fuelcell} - W_{pumps} - W_{blowers} \tag{3}$$

2.3.3. *Risk minimization*

Safety is another priority for the dehydrogenation module. The operating conditions and process design are expected to be adjusted for that purpose. Some authors have proposed some risk indicators to identify the most critical streams inside a process. This is the case of Shariff et al. (2012). There, an indicator is proposed based on the pressure, heating value and density of each stream and the flammability range. It is normalized based on the process average values and then an empirical constant is included to tighten the index results. On the other hand, other safety indicators, such as the Dow's Index Fire and Explosion, also take into account the quantity of combustible material in the process. Hence, a modification of the original index from Shariff et al. (2012) is proposed in Eq. 4. There, P and ΔFL are the stream pressure and the flammability range. Instead of employing average values, only a empirical constant (K_{SI}) is used. This is because the aim is not to identify critical streams but to penalize demanding operating conditions. Furthermore, to include the effect of the quantity of combustible material, the combustion enthalpy (H_c) is multiplied by the flowrate (F) of the specific stream instead of using the density. Since this index is applied across different operational loads, a Process Load factor (PLF) ranging from 0 to 1 (with 1 corresponding to 100% process load) is included.

For the calculation of the flammability range, values for standard conditions are taken for LOHCs and hydrogen. In the case of LOHCs these data are not available. Given the similar properties that these compounds may have with other fuels (e.g. diesel), the flammability range for them is taken as valid in this case. Then, the pressure and temperature dependence for flammability limits is introduced (Zabetakis, 1964; Planas-Cuchi et al., 1999).

$$SI = \frac{K_{SI} \cdot P \cdot \Delta FL \cdot \rho \cdot F \cdot H_c}{PLF} \tag{4}$$

The index proposed penalizes high pressures, flowrates, temperatures (as flammability range increases with it) and the most hazardous species. It is only calculated for the inlet and outlet streams from the reaction section after a brief process analysis. It is preferred to include only those streams that may present significant changes in the optimization. Other streams are not included for different reasons. For example, the initial LOHCs feed to the dehydrogenation module presents lower temperatures. The risks from the LOHCs recycle to the reaction section are already included in the inlet to the reaction section. Finally, the streams conditions (temperature, pressure and composition) in all the CHP streams are almost identical in all scenarios. Therefore, all these streams are not included in the final objective function presented in the Eq. 5. There, SI are the previously proposed safety index calculated for the inlet (i) and outlet (j) streams for the reaction section.

$$f_3 = \sum_{i=1}^{I} SI_i + \sum_{j=1}^{J} SI_j \tag{5}$$

Other works such as Martínez-Gomez et al. (2017) introduce the influence for each process equipment in the calculations. We left out on purpose the influence of process equipment. This is mainly because this process is based on conceptual process optimization which at the same time is on an early stage of development. There is a lack of data for the inherent risk for LOHCs reaction units considered as novel. In the case of other process units (heat exchangers, pumps, flash), only basic parameters are estimated and no accurate sizing is done (e.g., thickness, wide, length). It also complicates risk estimation. At this point, inherent process risk quantification shows up large uncertainty. In any case, we believe that our index is useful for safety purposes since it aims to minimize process operating conditions and combustible material in process streams. This is closely related to the consequences in the event of an accident.

2.3.4. *Equipment volume*

Equipment volume is a critical aspect for maritime transport. As a result, it is a relevant variable to perform optimization. The volume required to supply power demand can be divided into the process equipment (DH and CHP modules) and the energy carrier, in this case LOHCs. Note that the volume occupied by the LOHCs itself is considerably larger compared to equipment units. However, we consider that minimizing the equipment volume (EV) itself is also critical. This is because they require complex piping and instrumentation, safety distances, inspection or the layout may present some limitations. Since fuel volume strongly depends on other objective functions (LOHCs losses and fuel use efficiency), the fuel volume is left out on this case. Therefore, the optimization function consists in the Eq. 6, where the equipment volume is to be minimized. They include fuel cell, reactors and heat exchangers. The volume for other units is neglected.

$$f_4 = EV \tag{6}$$

2.4. *Constraints*

The optimization of this system is subjected to meet the power demand of the cargo ship. The net power produced with the fuel cell is obtained in Eq. 3. Then, an inequality constraint is imposed to produce at least the energy required for the ship. In the case of process design, 12 MW is imposed as constraint. For process operation, different constraint scenarios are evaluated (25%, 50%, 75%, 100%) based on base nominal power.

2.5. *Input variables*

In order to optimize the system, several input variables are evaluated. They are included in Table 1. The reactors are the core units of the dehydrogenation module. Therefore, it is paramount to optimize its operating conditions. These include the operating temperature (T) and pressure (P). In the case of the isothermal reactors, the heating oil (F_{oil}) used to control the temperature may have also a relevant impact. Typical temperature range for dibenzyltoluene dehydrogenation is 533-593 K (Preuster et al., 2018). However, higher conversions, limited by reaction equilibrium, are achieved at the highest temperature range (Dürr et al., 2021). At the same time, kinetics are also favored at these conditions. Therefore, 573-593 K temperatures are considered for the inlet of the reactors. The pressures for both reaction units are set up to 5 bar (Preuster et al., 2018). To avoid higher liquid evaporation and overcome the pressure drop in the reactors, intermediate 3 bar pressure is set as lower bound in the isothermal reactors. At this pressure, it is possible to achieve similar conversions compared to atmospheric conditions at higher temperatures according to Dürr et al. (2021) work. In the adiabatic units, the lower bound is reduced to 1.5 bar since lower LOHCs evaporation is expected. With regards to the heating oil flowrate, it is limited to 6 L/mol of fresh LOHC. This is to minimize LOHCs evaporation. Finally, other process parameters such as the amount of LOHCs introduced in the system (F_{LOHC}) or the recycle ratio of the final product (RR) are also included in this analysis. All these variables are used in both process design and operation optimization.

Table 1: Input variables for process optimization

Input variable	Value
$T_{isothermal}$	573.00-593.00 K
$P_{isothermal}$	3.00-5.00 bar
$D^2_{r,isothermal}/F_{LOHC}$	0.10-0.40 m^2/mol/s
$L_{isothermal}$	2.00-6.00 m
F_{oil}/F_{LOHC}	0.50-6.00 L/mol
$T_{adiabatic}$	573.00-593.00 K
$P_{adiabatic}$	1.50-5.00 bar
$D^2_{r,adiabatic}/F_{LOHC}$	0.10-0.40 m^2/mol/s
$L_{adiabatic}$	0.50-4.00 m
F_{LOHC}	10.00-30.00 mol/s
RR	0.00-66.67%
$n_{r,isothermal}$	1-2
$n_{r,adiabatic}$	0-2

Similarly, some design features for each reaction technology are also relevant. However, these are only considered as input variables for the process design stage. These include the length of the catalyst bed (L) and diameter (D). Different catalyst quantities are proposed for each of the reaction technologies. A higher temperature drop is expected in adiabatic units. As a result, lower bed size is expected compared to isothermal units. This is because reaction rate decreases and eventually the chemical equilibrium may be reached. Typical dimensions for a scrubbing unit for a 12 MW ship can be almost 9 m height and 3 m diameter (ABS, 2018). The size of the isothermal reactors is adapted to comparable dimensions. The reactor diameter for both technologies is adjusted to set the flowrate to have typical trickle bed reaction conditions (Satterfield, 1975). At the same time, the diameter is adjusted to minimize pressure drop.

Previous variables (operating conditions and design parameters) are continuous. However, it is also possible to evaluate the effect that integer variables may have in the process design optimization. This is the case of the number of isothermal and adiabatic units. Apart from the reaction units itself, the number of equipment for each reaction technology modifies the process superstructure. This is because intermediate heat exchangers and/or pumps are required between these technologies as shown in Figure 2. In this context, as introduced before, a detailed model is used to account for heat, mass and momentum transfer in the reaction units. This is essential to fully capture the effects of operating conditions, reactors design parameters and reaction technology selection on reaction progress.

2.6. Optimization algorithm: Bayesian Optimization

BO is employed for process design and operation optimization using different techniques. The general procedure includes a space-filling design, such as Sobol sampling with a reduced number of samples (n_0=10) to get initial dataset. Then, objectives and constraints are modeled using a ML model that outputs a probability distribution over outcomes, such as GP. Based on these GPs, acquisition function is maximized to get next point, which is evaluated. Finally, the dataset, D={$(x^i,y^i)_{i=1}^{n_d}$}, is updated and this process continues until the maximum number of iterations is reached (see Algorithm 1).

Algorithm 1 General BO algorithm.

1: **Initialize** Initial dataset D, Objective function f, Acquisition function Af, Domain Space X, Iterations I.
2: **for** $1, 2 \ldots I$ **do**
3: Train $GP(D)$ ▷ Training of GPs for objectives and constraints
4: $x^* \leftarrow \text{argmax}_{x \in X} Af(x)$ ▷ Maximize acquisition function to get new points
5: $y^* \leftarrow f(x^*)$ ▷ Evaluate new point
6: $D \leftarrow \{x^*, y^*\} \cup D$ ▷ Update the dataset
7: **end for**

However, some differences appear between the elements used in the different optimizations that are carried out in this work. The divergences between methods appear in: 1) Type of kernel used to model GPs (standard Radial Basis Function (RBF) or modified RBF) 2) Type of optimization (single or multiobjective) and 3) Optimizer used for acquisition function optimization (Continuous optimizer (CO), Mixed-Integer optimizer (MIO) or Evolutionary Algorithm (EA)). The differences between these approaches are detailed in the following and the different possibilities are depicted in Figure 4. Now, the different elements used in this work to perform BO are introduced.

2.6.1. Gaussian Process

GPs are used for the approximation of the objective functions and constraints. These are modeled using a mean function (m) and a covariance function ($k(\cdot,\cdot)$) as shown in Eq. 7.

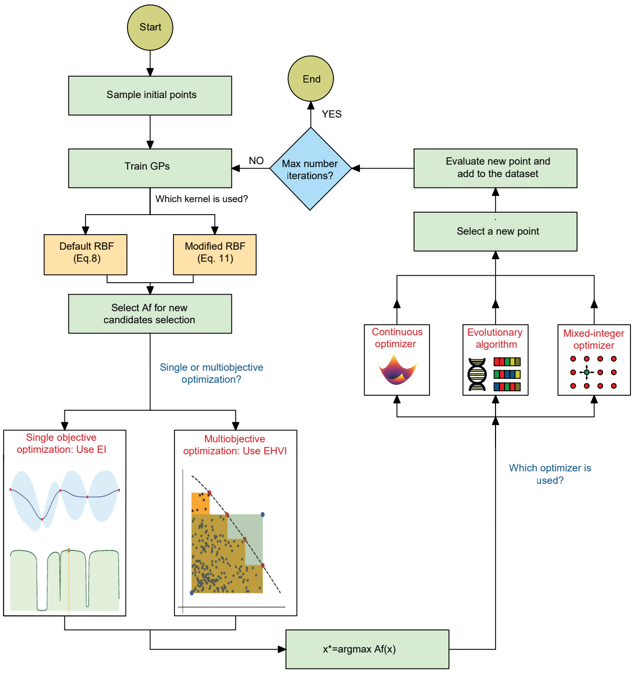

Figure 4: BO loop.

$$GP(m(\cdot), k(\cdot, \cdot)) \tag{7}$$

Constant zero mean is assumed to adjust mean function. To model covariance matrix, a standard RBF kernel may be used. The general formula is shown in Eq. 8. There, σ_f^2, refers to the variance of the process, $x \in \mathbb{R}^{n_x}$, the input vector for independent variables and $\Lambda \in \mathbb{R}^{n_x \times n_x}$ a matrix containing the inverse of squared lengthscale for each dimension on its diagonal.

$$k(\cdot, \cdot) = \sigma_f^2 \cdot \exp\left(-\frac{1}{2}(x - x)^T \Lambda (x - x)\right) \tag{8}$$

Note that noise term is removed. This is because function evaluations are noiseless since the results are based on process simulations. Lengthscale prior is based on log-normal distribution. Mean and standard deviation for this distribution take into account the scaling proposed in Hvarfner et al. (2024) work. For a given dataset, the posterior mean, μ_D, and posterior variance, σ_d^2, of the kernel can be computed using Eq. 9 and Eq.10 respectively. There, $\mathcal{K}$ represents the covariance function between the training dataset and itself, κ the covariance between the training dataset and a new point and y the set of dependent variables.

$$\mu_D(x|D) = m(x) + \kappa(x, X)\mathcal{K}^{-1}(X, X)(y - m(X)) \tag{9}$$

$$\sigma_D^2(x|D) = \kappa(x, x) - \kappa(x, X)^T\mathcal{K}^{-1}(X, X)\kappa(X, x) \tag{10}$$

The previous kernel is designed to work in a continuous variable space. However, significant discontinuities in the objective function may arise when integers are introduced in the formulation (process design optimization). In this work, two different strategies are proposed in the way kernel is defined if integers are present in the formulation:

1. Standard RBF Kernel (Eq. 8): Use the RBF kernel described above, with the integer variable rounded inside the function wrapper. This kernel is inherently continuous and does not account for the discontinuities caused by integer variables. However, ideally, there should be no distance between two non-integer values as they do not exist in the integer domain. According to Garrido-Merchán and Hernández-Lobato (2020), although rounding within the wrapper may outperform other strategies, such as rounding before function evaluation, it may still fail to capture the discontinuities introduced by integers in the formulation.
2. Modified RBF Kernel (Eq. 11): The previously described RBF kernel (including constraints, log-normal prior, constant mean) is replicated. However, the computation of distances between points is modified. The approach proposed in Garrido-Merchán and Hernández-Lobato (2020) is implemented for this purpose. This involves applying a transformation within the kernel to round integer variables, originally defined in the continuous space, to the closest integer. This way, no distance is measured between two points that round to the same integer value. Hence, both the mean and the confidence interval remain constant across the range of values that round to the same integer.

$$k(\cdot, \cdot) = \sigma_f^2 \cdot \exp\left(-\frac{1}{2}(\mathrm{round}(x) - \mathrm{round}(x))^T\Lambda(\mathrm{round}(x) - \mathrm{round}(x))\right) \tag{11}$$

2.6.2. *Acquisition function: Single and multiobjective optimization*

In this work, two types of optimizations are carried out: single and multiobjective optimization. Hence, different acquisition functions are used for each case: log-Expected Improvement (logEI) in single objective optimization and log-Expected Hypervolume Improvement (logEHVI) for multiobjective optimization (Figure 5 and 6 respectively). These are popular acquisition functions in the field of BO (Garnett, 2023; Fromer et al., 2024). The logEI acquisition function aims to balance exploration and exploitation by considering both the predicted mean and uncertainty. It selects new candidates that increase the likelihood of improvement by considering both the mean but also the uncertainty, see Eq. 12. There, $\mathrm{f}(\mathrm{x})$ and $\mathrm{f}_{\mathrm{best}}$ represent the objective evaluation for x and the best value found at the moment.

$$\mathrm{logEI}(\mathbf{x}|\mathrm{D}) = \log\left(\mathbb{E}[\max(0, \mathrm{f}(\mathrm{x}) - \mathrm{f}_{\mathrm{best}}))]\right) \tag{12}$$

Likewise, logEHVI tries to do so, but considers several objectives at once. In this case, a reference point is set and the non-dominated points are used to compute the hypervolume from it. In this work, the reference point is based on the worst results from each objective function from previous single objective optimization. The main idea of logEHVI approach, is to look for new feasible points that increase as much as possible this hypervolume and with the objectives, build the Pareto Front (Eq. 13). HV is the hypervolume and $\mathcal{P}$ the set of non-dominated solutions.

$$\mathrm{logEHVI}(\mathbf{x}|\mathrm{D}) = \log\left(\mathbb{E}[\max(0, \mathrm{HV}(\mathcal{P} \cup \mathrm{f}(\mathrm{x})) - \mathrm{HV}(\mathcal{P}))]\right) \tag{13}$$

2.6.3. *Acquisition function optimizers*

To obtain new points, several optimizers are proposed for the optimization of both acquisition functions. Automatic-differentiation optimizers can be used in a continuous space to maximize acquisition function and get new points. If no integers are present in the formulation, this option is used. However, when integer variables are present, derivatives cannot be computed for these variables. Then, in this work, for this situation, we looked at three possibilities: 1) use a CO, 2) use MIO which alternates between integer and continuous space or 3) use derivative-free EA optimizer.

2.6.4. *Implementation*

The BoTorch library is used to implement the BO loop. To implement the GPs for both objectives and constraints, SingleTaskGP from BoTorch, build on top of GPyTorch

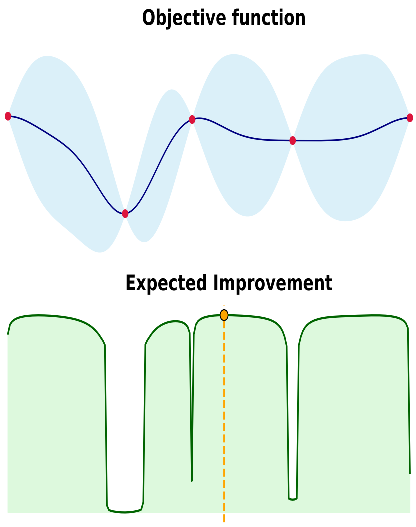

Figure 5: Expected Improvement acquisition function.

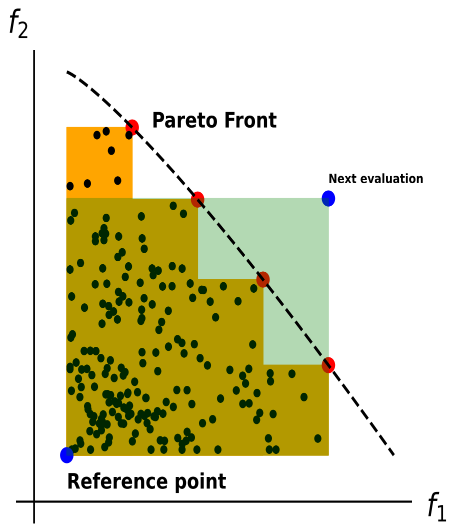

Figure 6: Expected Hypervolume Improvement acquisition function.

(Balandat et al., 2020; Gardner et al., 2018) is employed. At this point, two possible kernels can be used in this work:

1. Standard RBF: SingleTaskGP uses RBF kernel by default. Therefore, no modification is done to the covariance module.
2. Modified RBF: BoTorch allows the incorporation of integer distances in GPs for categorical variables using the Hamming Distance. However, it is not able to define distances between ordinal discrete values, which introduce discontinuities. The modified RBF presented in Eq. 11 is implemented by customizing the Kernel class from GPyTorch while the hyperparameters of the GPs are tuned using SingleTaskGP.

Both, acquisition functions, logEI and logEHVI for single and multiobjective optimization respectively, are implemented from BoTorch. Different optimizers were proposed for its optimization:

1. CO: For the optimization of acquisition function, optimize_acqf can be used with LBFGS-B as a continuous optimizer (Balandat et al., 2020).
2. MIO: For mixed spaces, optimize_acqf_mixed_alternating is also available and used. It alternates between LBFGS-B for continuous variables and local search for integer variables (Balandat et al., 2020).
3. EA: Finally, differential_evolution from scipy is implemented for an evolutionary algorithm (Virtanen et al., 2020).

2.6.5. Case studies

For the optimization of process design and operation, different BO techniques are used depending on the details of the optimization. These are summarized in this section. First, as introduced before, for process design, mixed-integer single and multiobjective constrained optimization is done. Due to the presence of integers, several strategies detailed before are evaluated. These are related to kernel use (use standard RBF or modified RBF kernel) and selection of the acquisition function optimizer (use CO, EA or MIO). The performance for each alternative has been compared with the others. Hence, the different case studies optimized for the design stage are included in Table 2.

Table 2: Case studies description for process design (D). Single Objective Optimization (S)/ Multiobjective Optimization (M). RBF (RBF Kernel Eq. 8)/MRBF (Modified RBF Kernel, Eq.11). CO (Continuous Optimizer)/EA (Evolutionary Algorithm)/ Mixed-Integer Optimizer (MIO).

Case Identifier	DS-RBF-CO	DS-MRBF-EA	DS-RBF-MIO	DS-MRBF-MIO	DM-RBF-CO	DM-MRBF-EA	DM-RBF-MIO	DM-MRBF-MIO
Objective functions	obj_{1-4}							
Constraints	Yes (12 MW)							
Optimization type	Single Objective				Multiobjective			
Acquisition function	qLogEI (Eq. 12)				qLogEHVI (Eq. 13)			
GP	RBF	Modified RBF	RBF	Modified RBF	RBF	Modified RBF	RBF	Modified RBF
Optimization approach	CO	EA	MIO	MIO	CO	EA	MIO	MIO

Likewise for process design, single and multiobjective optimization are performed for process operation. BO features are detailed in Table 3.

Table 3: Case studies description for process operation (O).

Case Identifier	OS-RBF-CO	OM-RBF-CO
Objective functions	obj_{3-4}	
Constraints	Yes (3-6-9-12 MW)	
Optimization type	Single Objective	Multiobjective
Acquisition function	qLogEI (Eq. 12)	qLogEHVI (Eq. 13)
GP	RBF	RBF
Optimization approach	CO	CO

3. Results

On this section, single and multiobjective optimization results are presented for process design stage. Then, after process equipment is set, operation optimization results are shown.

3.1. Process design

First, process design is optimized to set process equipment features. Hence, the optimization of single objectives is conducted for the mixed-integer space. Figure 7 shows how optimization progresses over BO iterations for each of the single objective optimization Cases presented in Table 2. Case DS-RBF-CO, based on standard RBF Kernel and continuous optimizer, shows clearly the worst performance compared to the others. Slower convergence and worse minimum values are found. The fact that neither RBF kernel nor optimizer took into account the presence of integers is the main reason to attribute this behavior. Despite that, investment function shows a comparable performance to other cases. This may be because the discontinuities that integer variables introduce to this objective function are less pronounced. With regards to the other Cases, either DS-MRBF-EA or DS-MRBF-MIO, which use Modified RBF and EA and MIO as optimizers respectively, present the best results at the end of the optimization for investment and volume. In the other two objectives, comparable results are found with DS-RBF-MIO (standard RBF combined with MIO). Moreover, a stepper descent is observed in fuel use efficiency and volume and comparable progress for risk and investment minimization with respect to DS-RBF-MIO. Note however, that it cannot be concluded that any of them is considerably better compared to DS-RBF-MIO. This may be due to the reduced integer space and number of integer variables. However, it may be possible to find higher differences when both increase. Finally, the results for the best points found for each objective function are presented in Table 4. Beyond process optimization, the use of detailed reactor models enables the representation of relevant phenomena during LOHCs dehydrogenation, thereby incorporating their effects into reactor design, configuration, and operating conditions selection.

Table 4: Optimization results for the design stage.

Objective	f_1	f_2	f_3	f_4	MO ($f_{1,2,3,4}$)
f_1 (MM$)	26.96	29.86	33.36	30.00	27.35
f_2(%)	32.90	43.47	27.06	18.38	37.49
f_3 (RU)	3.54	2.92	1.57	3.35	2.26
f_4 (m^3)	61.29	101.65	120.42	52.86	71.36
$T_{isothermal}$ (K)	593.00	574.43	593.00	590.82	580.11
$P_{isothermal}$ (bar)	3.00	4.31	3.00	3.77	3.00
$D^2_{r,isothermal}/F_{LOHC}$ (m^2/mol/s)	0.40	0.40	0.37	0.10	0.27
$L_{isothermal}$ (m)	2.00	5.91	5.88	3.00	5.00
F_{oil}/F_{LOHC} (L/mol)	5.45	6.00	1.43	2.26	3.19
$T_{adiabatic}$ (K)	593.00	593.00	580.74	593.00	590.68
$P_{adiabatic}$ (bar)	1.50	1.50	1.50	1.50	1.50
$D^2_{r,adiabatic}/F_{LOHC}$ (m^2/mol/s)	0.10	0.21	0.10	0.10	0.10
$L_{adiabatic}$ (m)	0.50	4.00	4.00	0.50	0.86
F_{LOHC} (mol/s)	16.76	12.68	20.38	30.00	14.71
RR (%)	66.67	66.67	0.00	66.67	66.67
$n_{r,isothermal}$	2	2	2	1	2
$n_{r,adiabatic}$	2	2	2	2	2

The single objective results are opposed between different optimizations. For exam-

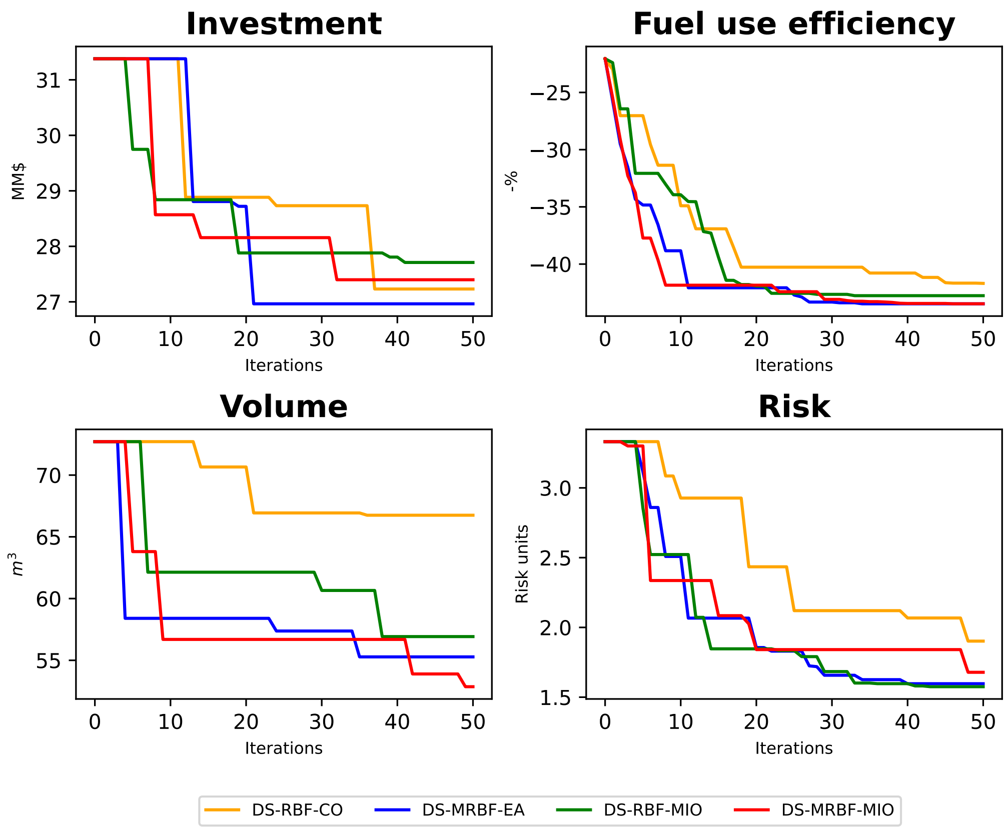

Figure 7: Mixed-integer single objective optimization.

ple, higher temperatures and lower pressures favor reaction kinetics and dehydrogenation equilibrium. However, at the same time, higher LOHCs evaporation is expected for these conditions. In the case of investment and equipment volume minimization, it is preferred to set high temperatures and low pressures in the isothermal reactors in spite of liquid evaporation. However, to maximize fuel use efficiency, it is preferred to increase pressure and reduce temperature to minimize evaporation phenomena.

Finally, lower pressures are set in the isothermal and adiabatic reactors for risk minimization. However, higher temperature is preferred in isothermal reactors, to increase hydrogen production, and intermediate temperature conditions are set in adiabatic units. In contrast, for the other objectives, lower pressures and higher temperatures are set in adiabatic units. This is because adiabatic reactors are less likely to LOHCs evaporation because of the adiabatic operation. With regards to LOHCs recycle, high values are beneficial for all objectives except for risk minimization. This is because it increases hydrogen production but at the same time there exists a higher LOHCs flowrate. Hence, it is set to the upper bound in these cases and no recycle is found for risk minimization. Moreover, significant differences can be seen in terms of LOHCs use. While fuel use efficiency sets a low value to maximize LOHCs conversion, other objectives such as volume minimization increase it considerably. This is because of better mass and heat transfer or the use of higher reactant concentrations. This results in lower catalyst requirements.

Overall, the variables that most strongly influence the shift between objectives are the fresh LOHCs feed, the use of oil, the operating conditions of the isothermal reactors (pressure and temperature), the recycle ratio, and the reactor dimensions. Investment cost and equipment volume tend to align in their preferred operating conditions for both isothermal and adiabatic units, mainly to reduce catalyst consumption. However, notable differences arise regarding LOHCs utilization. For volume minimization, higher LOHCs flow rates are selected to reduce reactor size since they promote higher reaction rates. At the same time, it reduces the need for oil compared with the investment optimization. In contrast, investment function penalizes excessive LOHCs consumption. Despite this, both strategies favor smaller adiabatic and isothermal reactor dimensions. The similarity in process configurations for these two objectives highlights a degree of interdependence between them.

In contrast, the fuel-use efficiency and risk objectives promote substantially different trends. To maximize efficiency, the system tends to operate at higher pressures and lower temperatures to avoid LOHCs evaporation, while favoring lower fresh LOHCs usage, high recycle ratios to increase conversion, and extensive use of heating oil to maintain a stable reactor temperature. Risk minimization, however, prioritizes reducing the operating conditions and total amount of combustible material in the system, which leads to choosing lower operating conditions, limiting recycle and use of oil, and increasing reactor size.

An additional source of conflict arises from the integer decision variables associated with the process layout. For the volume-minimization objective, the optimal configuration selects two adiabatic reactors and only one isothermal reactor, reducing total equipment volume. This is attributed to the bigger size of isothermal units compared to adiabatic ones. However, for the other objectives, the optimization consistently selects two isothermal and two adiabatic units, since increasing the number of isothermal reactors enhances temperature control, conversion and safety margins. This difference highlights how discrete design choices can shift the trade-offs among objectives.

This previous process assessment is complemented with a quantitative analysis provided in the Supporting Information. There, a Spearman partial correlation matrix is presented for all feasible process design experiments to identify the interactions between process variables and each objective, as well as the interactions among the objectives themselves. Since partial correlations may overlook relevant variables due to inter-variable dependencies or the limited number of experiments, the Gaussian Process (GP) kernel lengthscales are also reported, as they indicate the relative influence of each variable on the objective functions. The analysis shows that a higher use of fresh LOHCs leads to lower fuel efficiency and higher equipment volume, primarily due to an increase in reactor diameter associated with the higher mass flow. However, increasing LOHCs loading also enhances reaction rates and catalyst utilization, which in turn shortens the required reactor length to meet hydrogen demand, mitigating the volume increase. Both the diameter and length of the isothermal reactors were found to have a strong relationship with total equipment volume. Recycle ratio and oil consumption are associated with higher process risk, while the expected relationship between equipment volume and investment cost is also confirmed. Finally, some variables such as isothermal reaction conditions or the number of units do not show strong correlations with the objectives in the Spearman matrix. However, their low GP lengthscales indicate a substantial non-linear influence on the objective values, demonstrating their importance even when not captured by the correlation analysis.

Then, multiobjective optimization is carried out. The metric used to measure the performance for each case is the hypervolume. To perform this optimization, 5 runs are done for each case. This is because randomness of BO algorithm has an impact on its performance because of its stochastic nature. Thus, the same seeds are fixed and shared between Cases to run the simulations. This way, optimization progress is provided in Figure 8 showing the minimization of the negative hypervolume. The shading represents the interval between minimum and maximum values of the hypervolume for each iteration. Then, the mean value is represented with a line.

As in previous single objective optimization, combination of continuous RBF Kernel and continuous optimizer (DM-RBF-CO) presents the worst performance. This shows again the benefits of considering the mixed-integer space. With regards to the other cases, DM-MRBF-MIO seems to perform slightly better followed by DM-MRBF-EA. Both use modified RBF. However, the differences are not large enough to assure DM-MRBF-MIO and DM-MRBF-EA outperform DM-RBF-MIO. In any case, these results indicate that if integers are present in the formulation, the mixed-integer space approaches at least perform similar (if not better) compared to continuous space approaches. With regards to the use of optimizers, in previous single objective optimization it was not possible to conclude which option was better. However, MIO showed a small improvement compared to EA for multiobjective optimization.

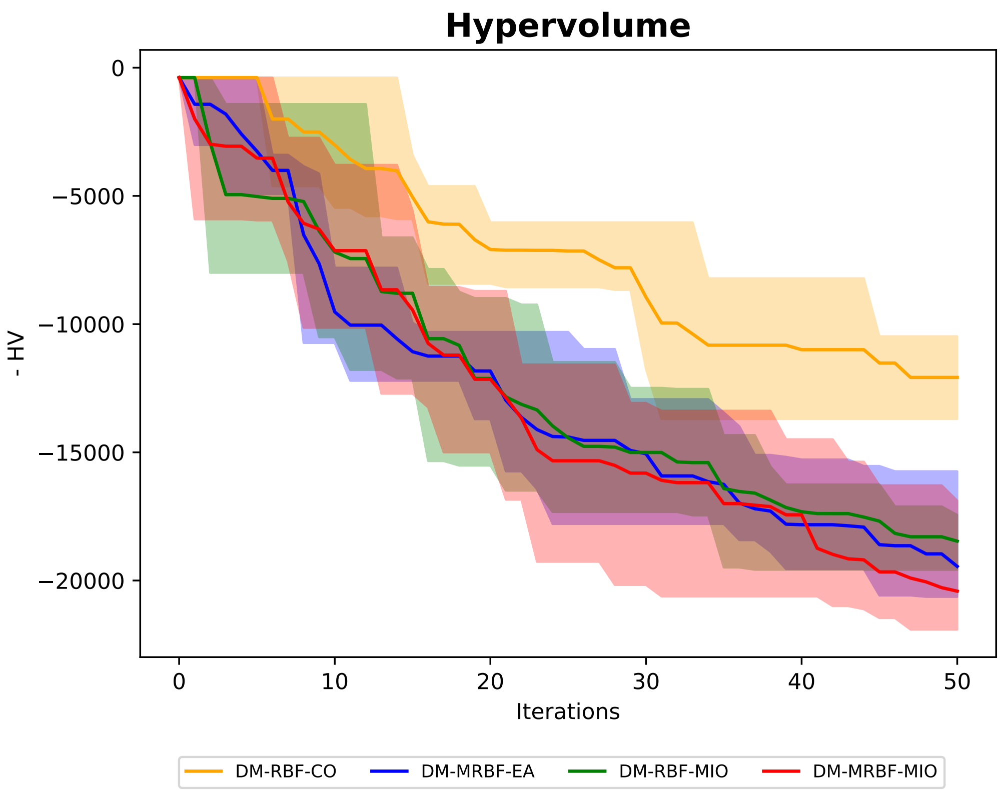

Figure 8: Mixed-integer multiobjective optimization.

At this point, several feasible candidates are obtained from multiobjective optimization. The non-dominated solutions define the Pareto Front. To determine the final process design, the Utopia Point methodology described above is applied. The results of the single-objective optimizations are used to define the Utopia Point, and the non-dominated solution exhibiting the minimum Euclidean distance to this point is selected. The results from this candidate are included in Table 4. It is shown how intermediate values are obtained for all the objectives.

In this study, a three-phase reactor model based on previous work is employed for the analysis of LOHCs dehydrogenation in both adiabatic and isothermal reactors (Prieto et al., 2023). The model accounts for mass, heat, and momentum transfer, as well as vapor-liquid equilibria, pressure drop, liquid holdup, and catalyst wetting effects among other phenomena. The detailed model can be found in the Supporting Information document. The importance of considering them is based on reaction units scale-up and the complexity of multiphase systems. In the present work, the impact of these effects on reactor performance is quantitatively demonstrated through direct comparison with simplified reactor modeling.

To this end, two baseline models of reduced complexity are introduced. As a first baseline, LOHCs process conversion is estimated assuming thermodynamic equilibrium, using the equation proposed by Dürr et al. (2021) thereby neglecting kinetic and transport limitations. As a second baseline, intrinsic kinetics are employed in a reduced reactor model in which mass and heat transfer resistances, vapor-liquid equilibria, pressure drop, liquid holdup, and catalyst wetting effects are omitted. For that purpose, intrinsic kinetics proposed by Geißelbrecht et al. (2024) are used, while other reactor modeling elements described in the same work are not considered.

The process conversions predicted by these simplified models are compared against those obtained using the full three-phase reactor models under identical process design and operating conditions. This comparison enables a quantitative assessment of the influence of the neglected phenomena on reactor and process performance. It is found that the equilibrium-based baseline overestimates LOHCs process conversion by 27-156%, while the kinetics-only baseline overpredicts LOHCs process conversion by 20-120% depending on the design and operating conditions. These deviations can be attributed to the omission of relevant physical effects such as liquid evaporation, pressure drop, and heat transfer limitations among others.

The importance of using detailed reactor models lies in their ability to capture phenomena that strongly influence unit design and operating conditions. Simplified baseline models fail to account for key effects such as reactor diameter, which significantly affects gas and liquid velocities and, consequently, pressure drop, heat and mass transfer, holdup, and catalyst wetting efficiency. Similarly, the influence of pressure and temperature is not fully captured, as liquid evaporation or pressure drop, both critical phenomena, are neglected. As a result, simplified models overestimate LOHCs conversion, leading to underestimated catalyst requirements, reducing equipment volume and investment costs. They also underestimate process energy requirements and risk, as fresh LOHCs flowrates and pumping energy would be reduced and evaporation losses are not considered. In the case of isothermal multitubular reactors, the influence of the heating agent flowrate is not accounted for. Assuming ideal isothermal operation neglects variations in reaction and evaporation rates along the reactor and possible temperature fluctuations. Additionally, the choice of the number of reaction units has a reduced impact due to the assumption of isothermal and adiabatic operation and the absence of liquid evaporation.

With regards to the feasibility of LOHCs use for maritime applications, the volume that equipment occupies is manageable regarding typical ship dimensions. At the same time, it is possible to use the energy stored in LOHCs to convert into electricity with a yield above 35%. The electrical efficiency of using hydrogen in the SOFC reaches almost 55%. However, the use of power in air blowers and pumps, AC to DC conversion or incomplete conversions of LOHCs reduce it. Then, with a higher conversion of LOHCs it is possible to improve the energy density of this system. It would be possible to implement some LOHCs reuse techniques as proposed in Gambini et al. (2024b) or mix fresh LOHCs with the final product. However, the study of these strategies is out of the scope of this work. Considering the LOHCs conversion for the design point and the hydrogen requirements from the journey presented in Gambini et al. (2024a), the LOHCs volume would be 776.5 m^3. This is considerably larger compared to process equipment (71.36 m^3). However, minimizing process units volume is critical since safe distances, piping and equipment layout must be considered as well.

For comparison purposes, compressed or liquified hydrogen fuel would occupy 822 and 463 m^3 respectively based on their storage conditions. However, other significant problems may arise for these technologies. For example, liquefaction technology must reduce boil-off losses and provide insulation to the tanks in the cargo ship. At the same time, high energy consumption is attributed to this technology for its storage, while LOHCs are able to provide energy demand using SOFC exhaust heat. With regards to compressed hydrogen, 700 bar pressure, poses a challenge in the operation and safety of these systems. At the same time, a high cost is attributed to these tanks (850 \$/kg). For this situation it would reach approximately 28 MM\$ (Reuß et al., 2017).

The trade-off between the presented functions ($obj_{1,2,3,4}$) is achieved at high-intermediate temperatures and lower pressures for both reaction technologies. At the same time, low-medium reactor sizes are suggested and intermediate use of fresh LOHCs and heating oil. Finally, the distribution of investment and volume for each type of equipment (excluding LOHCs storage tanks), are shown in Figure 9.

In the case of DH module, dehydrogenation reactors and LOHCs replacement represent the most significant contributions in terms of costs. The cost of the reactors is around 126.80 $\$/kW_{H_2,LHV}$. The correlation proposed by Eypasch et al. (2017) is used an updated to the same basis of this work. A similar value is obtained for the investment of the reaction section (136.05 $\$/kW_{H_2,LHV}$). Other units such as heat exchangers or rotating equipment, represent around 20% of the investment in this module. With regards to equipment volume, reactors have a significant impact on this area. For the CHP module, fuel cell clearly holds the higher volume fraction and is also the main source of investment. However, compressors (air blower) and the burner also present a contribution. Finally, considering the two systems together, the total investment cost of the system represents 1990 $\$/kW_{el}$ (excluding LOHCs losses). The fuel cell has the

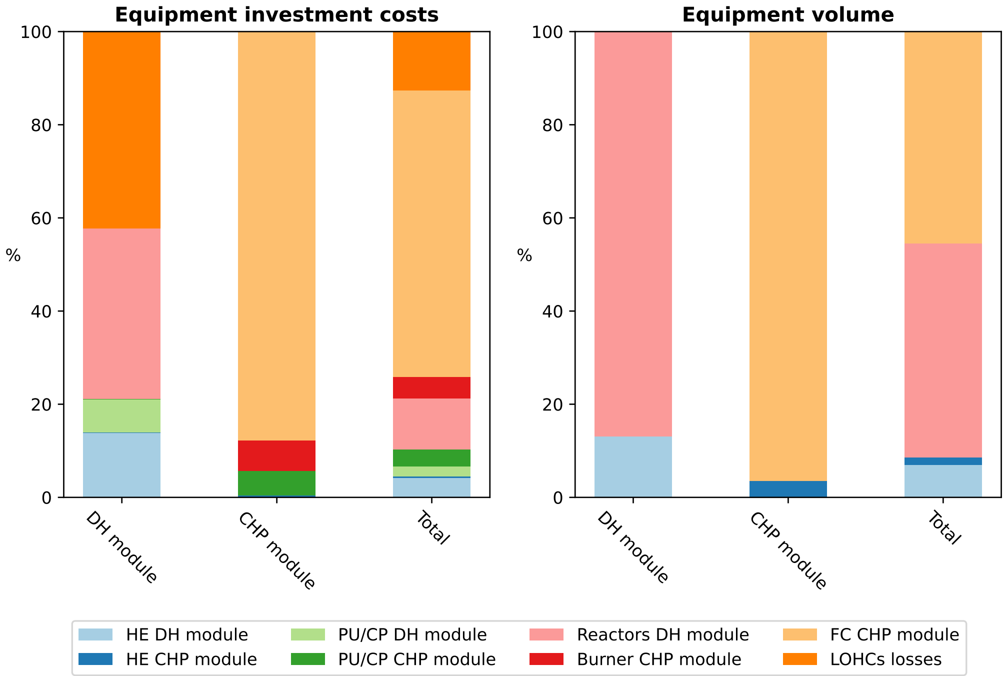

Figure 9: Equipment investment and volume distribution. HE (Heat Exchanger), PU (pump), CP (compressor), FC (fuel cell).

highest impact in terms of investment. Nevertheless, similar volumes are expected for dehydrogenation reactors and fuel cell.

3.2. Process operation

Once process design features are set based on previous multiobjective optimization, process operation can be optimized for different energy demands (25, 50, 75, 100%). The problem formulation constraints are adapted conveniently for each situation. First, single objective optimization is performed (OS-RBF-CO). Then, with these results, reference point is set and then multiobjective (OM-RBF-CO) for risk minimization and fuel use maximization is done. Note that in both cases all input variables are continuous. Therefore, only RBF Kernel and CO are used.

The results for these optimizations are shown in Table 5. As in the previous stage, the point selection for multiobjective optimization considers the minimum Euclidean distance with respect to the Utopia Point. However, note that there exists a wide range of possibilities as shown in Figure 10. There, the Pareto Front for each of the energy demand cases is represented together with the single objective optimization results. Note that multiobjective BO procedure is able to build an evenly distributed set of solutions between the single objective results. It clearly shows that the optimization procedure between both objectives is balanced. At the same time, the selection for the operational points is found in a narrow range. The fuel efficiency and risk vary up to 10% for MO results. These variations are attributed to a higher catalyst-to-LOHCs relationship, that provides the system flexibility to improve the efficiency and/or minimize process risk. Likewise, the similarities between results occur along the Pareto Fronts for all operational loads. The differences are attributed to the same reason detailed before. Hence, this shows that although process design and then operation have been optimized using a sequential approach, there is a great interdependence between the operation under nominal conditions and other reduced loads. In any case, if the differences would increase between operational loads and if optimization was done for a specific route, then, other approaches may be used such as design under uncertainty or multi-scenario design. However, note that in this work no specific route has been considered and the optimization of a standard ship power system has been done. At the same time, even for the same journey, cargo ship power load profiles vary considerably due to several reasons (e.g., weather conditions, charge). Therefore, it is preferred to demonstrate the feasibility of the operation under different loads and the great influence that nominal conditions have over other reduced loads.

As in the previous design stage, the operating conditions for the isothermal reactor, the recycle ratio, and the fresh LOHCs feed are the variables showing the most significant conflicts between risk minimization and fuel-use efficiency. Therefore, it is reasonable to adjust these variables when selecting the operating point, depending on the priority assigned to each objective in a given case, either to reduce operating conditions and total material flow (to lower inherent process risk) or to favor higher conversions. The final selection shows a trade-off between both risk and fuel use efficiency functions. However, in any of them needs to be favored, it is possible to select another operating point. The results show that for the fuel use efficiency, values should range between 25-40%. In terms of LOHCs conversion this would represent final conversions ranging from 50-80% considering nearly 50% system electrical efficiency. This range of conversions is found within the values proposed by other works (Gambini et al., 2024a).

While fuel use efficiency optimization favors high recycle, use of hot oil and low LOHCs flowrate, risk minimization promotes the opposite. Although it can be contradictory, a higher amount of fresh LOHC favors risk reduction. This is because it reduces the need for recycling and hot oil to meet hydrogen demand since higher reactant concentration favors better catalyst use. However, this negatively affects LOHCs conversion. To reach a trade-off between both objectives intermediate values are found for these three variables.

Table 5: Optimization results for the operation stage.

Load	25%			50%			75%			100%		
Objective	f_2	f_3	MO ($f_{1,2}$)	f_2	f_3	MO ($f_{1,2}$)	f_2	f_3	MO ($f_{1,2}$)	f_2	f_3	MO ($f_{1,2}$)
f_2 (%)	43.09	26.05	37.73	42.28	26.00	36.56	42.17	22.53	37.83	40.82	22.65	34.87
f_3 (RU)	2.72	1.72	1.92	2.52	1.70	1.90	3.09	1.57	2.07	2.94	1.67	1.95
$T_{isothermal}$ (K)	577.07	584.22	593.00	573.00	593.00	584.38	584.69	593.00	593.00	573.00	593.00	592.91
$P_{isothermal}$ (bar)	3.45	3.00	3.00	3.00	3.00	3.00	3.99	3.00	3.00	3.94	3.00	3.00
$\frac{F_{oil}}{F_{LOHC}}$ (L/mol)	5.19	1.42	3.19	4.50	1.30	3.07	6.00	0.96	3.24	5.45	1.12	2.75
$T_{adiabatic}$ (K)	593.00	593.00	593.00	593.00	593.00	593.00	593.00	593.00	593.00	593.00	593.00	593.00
$P_{adiabatic}$ (bar)	1.50	1.50	1.50	1.50	1.50	1.50	1.50	1.50	1.50	1.50	1.50	1.50
F_{LOHC} (mol/s)	3.19	5.20	3.65	6.52	10.61	7.54	9.81	18.35	10.93	13.51	24.34	15.81
RR (%)	66.67	0.00	10.80	66.67	0.00	0.19	66.67	0.00	36.31	66.67	0.00	47.16

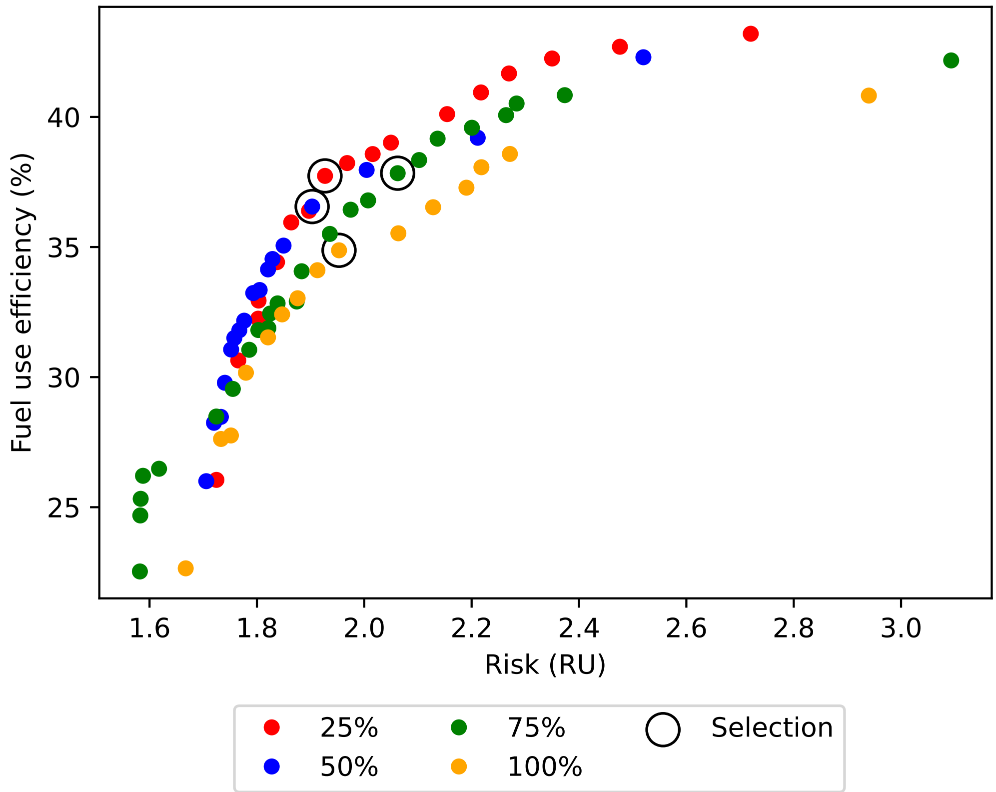

Figure 10: Fuel use efficiency and risk results using multiobjective optimization for different energy demands.

The pressure and temperatures conditions for adiabatic trickle beds are set to the lower and upper bounds respectively in all cases. Hence, a higher reaction rate is promoted while evaporation is reduced in adiabatic units. Similarly, pressures are set to lower bounds in isothermal units, although in some cases for fuel use maximization, intermediate values are used to minimize evaporation. Based on the same reason, intermediate temperatures are also established for the single objective optimization of this function.

With regards to the effect of the process load on the objective functions, a slight increase is possible at lower load values for the maximum higher fuel use efficiency (up to 43.09 %). The system is oversized, and then, it is possible to achieve higher LOHCs conversions. In the case of risk minimization, only slight variations are observed for MO, with a small improvement at lower loads compared to nominal conditions. However, under single-objective optimization, heating oil flowrate (in the lower part of its range), increases to compensate for the reduced LOHCs feed to the reactors, which negatively influences reaction progress, thereby raising risk index in single objective optimization for the lower operating loads.

4. Conclusions

In this work, LOHCs use for hydrogen storage in maritime applications is assessed. LOHCs process design and operation were optimized considering operating and design parameters together with the selection of two reaction technologies: isothermal and adiabatic reactors. The ship load profile was not considered in the process design optimization. However, in future work, for a specific vessel with a predefined route, incorporating its load profile could be of interest.

Modeling these three-phase reactors required from detailed mass, heat and momentum representation. A quantitative comparison was done against simplified baselines, showing that if relevant phenomena are omitted, reactor performance is considerably overestimated. The selection and number for each one were also considered in the optimization. For that purpose, BO has been applied for single/multiobjective, mixed-integer constrained optimization. Specifically, the presence of integers, which introduced discontinuities, is regarded as a challenge for optimization. One of the main contributions to this work is the use of specific strategies to handle integers. Therefore, different strategies were analyzed to perform mixed-integer optimization. These included the modification of standard RBF kernel and the use of different optimizers for the acquisition functions.

First, process design single (investment, volume, fuel use and risk) and then multi-objective optimizations were carried out. Process design set 2 isothermal and 2 adiabatic reactors with medium size. For the proposed design, a trade-off was reached between investment (27.35 MM$), equipment volume (71.36 m^3), fuel use efficiency (37.49 %) and risk minimization (2.26 RU). The results from process design suggest the use of intermediate or high temperatures and low pressures for the reactors, high recycle ratio and intermediate use of LOHCs and hot oil.

The optimization procedure showed in single and multiobjective optimizations that integers variables should be taken into consideration when using BO. DS-RBF-CO and DM-RBF-CO cases (RBF kernel+ CO), showed the worst results compared to the other approaches. On the other hand, although it could not be concluded that the GP kernel modification combined with different optimizers can clearly outperform DS-RBF-MIO and DM-RBF-MIO (RBF kernel + MIO), the optimizations reached either better or similar results. This is attributed to GP modification is able to capture better the discontinuities. Hence, the approaches applied in this work are regarded as promising to perform mixed-integer optimization.

Finally, operation was optimized for different capacities and similar operating strategies compared to process design were selected to find a trade-off between risk minimization and fuel use maximization. However, if other operating points are selected, it is also possible to prioritize either fuel use efficiency (up to 43.09 %) or risk minimization. Therefore, this work contributes to the LOHCs development and process design optimization in mixed-integer spaces using BO.

Acknowledgments

The authors acknowledge the support from the Ministry of Science and Innovation MICIN (PID2023-146231OB-I00) and the FPU, Spain grant (FPU21 /02413) to C.P.

Nomenclature

A_f	Acquisition function
B	Burner
BO	Bayesian Optimization
CHP	Combined Heat and Power
CO	Continuous Optimizer
CP	Compressor
D	Dataset
d_t	Tube diameter (m)
D_r	Reactor diameter (m)
DH	Dehydrogenation
DoDH	Degree of dehydrogenation
E	Energy (kJ)
EA	Evolutionary Algorithm
EI	Expected Improvement

EHVI	Expected Hypervolume Improvement
EIC	Equipment Investment Cost (MM$)
EV	Equipment Volume (m^3)
f	Objective function
F	Flowrate (mol/s)
FC	Fuel Cell
FL	Flammability limits (%)
GP	Gaussian Process
$\mathrm{H_c}$	Combustion enthalpy (kJ/mol)
HE	Heat Exchanger
HV	Hypervolume
$\mathrm{k_p}$	Polytropic constant
$\mathrm{K_{SI}}$	Safety index empirical constant
i	Inlet stream index
I	Iterations
IMO	International Maritime Organization
j	Outlet stream index
k	Covariance function
L	Reactor length (m)
m	Mean function
MIO	Mixed-Integer Optimizer
ML	Machine Learning
MO	Multiobjective
MRC	Material Replacement Cost (MM$)
MX	Mixer
n_r	Number of reactor
NP	Net power (MW)
P	Pressure (bar)
PU	Pump
R	Reactor
RR	Recyle ratio (%)
RBF	Radial Basis Function
SI	Safety index
SO	Single Objective
SOFC	Solid Oxide Fuel Cell
T	Temperature (K)
LOHCs	Liquid Organic Hydrogen Carriers

VL	Valve
W	Power (MW)
x	Independent variables
$\mathcal{X}$	Domain space
y	Dependent variables
Λ	Inverse squared lengthscale matrix
μ_{D}	Posterior mean
$\mathcal{P}$	Set of non-dominated solutions in multiobjective optimization
σ_{f}^2	Variance of the process
σ_{D}^2	Posterior variance
ρ	Stream density ($\mathrm{kg/m^3}$)
$\mathcal{K}$	Covariance between training dataset and itself
κ	Covariance between training dataset and a new point

References

Abdin, Z., Tang, C., Liu, Y., Catchpole, K., 2021. Large-scale stationary hydrogen storage via liquid organic hydrogen carriers. iScience 24, 102966. URL: https://www.sciencedirect.com/science/article/pii/S2589004221009342, doi:https://doi.org/10.1016/j.isci.2021.102966.

ABS, 2018. ABS advisory on exhaust gas scrubber systems. Technical Report. American Bureau of Shipping (ABS).

Amini, S., Vannieuwenhuyse, I., Morales-Hernández, A., 2024. Constrained bayesian optimization: A review. IEEE Access .

Balandat, M., Karrer, B., Jiang, D.R., Daulton, S., Letham, B., Wilson, A.G., Bakshy, E., 2020. BoTorch: A Framework for Efficient Monte-Carlo Bayesian Optimization, in: Advances in Neural Information Processing Systems 33. URL: http://arxiv.org/abs/1910.06403.

Baldea, M., Endler, E.E., Hale, E., Maravelias, C.T., Barolo, M., Harjunkoski, I., Mercangoz, M., Shah, S.L., Soroush, M., Young, B.R., Zhang, Q., 2025. Transforming the process industries through electrification: Challenges and opportunities. Industrial & Engineering Chemistry Research 64, 16466–16478. doi:10.1021/acs.iecr.5c01256.

Bartoli, N., Lefebvre, T., Lafage, R., Saves, P., Diouane, Y., Morlier, J., Bussemaker, J., Donelli, G., de Mello, J.M.G., Mandorino, M., Vecchia, P.D., 2025. Multi-objective bayesian optimization with mixed-categorical design variables for expensive-to-evaluate aeronautical applications. URL: https://arxiv.org/abs/2504.09930, arXiv:2504.09930.

Couper, J.R., 2005. Chemical process equipment: selection and design. volume 6. Gulf professional publishing.

Diessner, M., Wilson, K.J., Whalley, R.D., 2024. On the development of a practical bayesian optimization algorithm for expensive experiments and simulations with changing environmental conditions. Data-Centric Engineering 5, e45. doi:10.1017/dce.2024.40.

Distel, M.M., Margutti, J.M., Obermeier, J., Nuß, A., Baumeister, I., Hritsyshyna, M., Weiß, A., Neubert, M., 2025. Large-scale h2 storage and transport with liquid organic hydrogen carrier technology: Insights into current project developments and the future outlook. Energy Technology 13, 2301042. URL: https://onlinelibrary.wiley.com/doi/abs/10.1002/ente.202301042, doi:https://doi.org/10.1002/ente.202301042.

Dürr, S., Zilm, S., Geißelbrecht, M., Müller, K., Preuster, P., Bösmann, A., Wasserscheid, P., 2021. Experimental determination of the hydrogenation/dehydrogenation - equilibrium of the lohc system h0/h18-dibenzyltoluene. International Journal of Hydrogen Energy 46, 32583–32594. URL: https://www.sciencedirect.com/science/article/pii/S0360319921027841, doi:https://doi.org/10.1016/j.ijhydene.2021.07.119.

Eypasch, M., Schimpe, M., Kanwar, A., Hartmann, T., Herzog, S., Frank, T., Hamacher, T., 2017. Model-based techno-economic evaluation of an electricity storage system based on liquid organic hydrogen carriers. Applied Energy 185, 320–330. URL: https://www.sciencedirect.com/science/article/pii/S0306261916315094, doi:https://doi.org/10.1016/j.apenergy.2016.10.068.

Fromer, J.C., Graff, D.E., Coley, C.W., 2024. Pareto optimization to accelerate multi-objective virtual screening. Digital Discovery 3, 467–481. URL: http://dx.doi.org/10.1039/D3DD00227F, doi:10.1039/D3DD00227F.

Gambini, M., Guarnaccia, F., Di Vona, M.L., Manno, M., Vellini, M., 2022. Liquid organic hydrogen carriers: Development of a thermodynamic and kinetic model for the assessment of hydrogenation and dehydrogenation processes. International Journal of Hydrogen Energy 47, 28034–28045. URL: https:

//www.sciencedirect.com/science/article/pii/S0360319922027525, doi:https://doi.org/10.1016/j.ijhydene.2022.06.120.

Gambini, M., Guarnaccia, F., Manno, M., Vellini, M., 2024a. Feasibility study of lohc-sofc systems under dynamic behavior for cargo ships compared to ammonia alternatives. International Journal of Hydrogen Energy 81, 81–92. URL: https://www.sciencedirect.com/science/article/pii/S0360319924028982, doi:https://doi.org/10.1016/j.ijhydene.2024.07.224.

Gambini, M., Guarnaccia, F., Manno, M., Vellini, M., 2024b. Flow rate control in a plug-flow reactor for liquid organic hydrogen carriers dehydrogenation. International Journal of Hydrogen Energy 62, 375–388. URL: https://www.sciencedirect.com/science/article/pii/S0360319924009145, doi:https://doi.org/10.1016/j.ijhydene.2024.03.082.

Gardner, J.R., Pleiss, G., Bindel, D., Weinberger, K.Q., Wilson, A.G., 2018. Gpytorch: Blackbox matrix-matrix gaussian process inference with gpu acceleration, in: Advances in Neural Information Processing Systems.

Garnett, R., 2023. Bayesian optimization. Cambridge University Press.

Garrido-Merchán, E.C., Hernández-Lobato, D., 2020. Dealing with categorical and integer-valued variables in bayesian optimization with gaussian processes. Neurocomputing 380, 20–35. URL: https://www.sciencedirect.com/science/article/pii/S0925231219315619, doi:https://doi.org/10.1016/j.neucom.2019.11.004.

Geißelbrecht, M., Benker, R., Seidel, A., Preuster, P., 2024. Modeling of the continuous dehydrogenation of perhydro-dibenzyltoluene in a cuboid reactor. Energy Technology 12, 2300813. URL: https://onlinelibrary.wiley.com/doi/abs/10.1002/ente.202300813, doi:https://doi.org/10.1002/ente.202300813.

Gómez-Castro, F.I., Rico-Ramírez, V., 2025. Optimization in Chemical Engineering: Deterministic, Meta-heuristic and Data-driven Techniques. Walter de Gruyter GmbH & Co KG.

Heublein, N., Stelzner, M., Sattelmayer, T., 2020. Hydrogen storage using liquid organic carriers: Equilibrium simulation and dehydrogenation reactor design. International Journal of Hydrogen Energy 45, 24902–24916. URL: https://www.sciencedirect.com/science/article/pii/S0360319920317110, doi:https://doi.org/10.1016/j.ijhydene.2020.04.274.

Hvarfner, C., Hellsten, E.O., Nardi, L., 2024. Vanilla bayesian optimization performs great in high dimensions. URL: https://arxiv.org/abs/2402.02229, arXiv:2402.02229.

Hydrogen Europe, 2021. How hydrogen can help decarbonise the maritime sector .

Hydrogenious Maritime, 2023. Enabling hydrogen to the maritime industry. URL: https://www.hydrogenious-maritime.com/.

ICCT, I.C.o.C.T., 2020. Vision 2050: a strategy to decarbonize the global transport sector by mid-century. white paper .

Iwama, R., Kaneko, H., 2021. Design of ethylene oxide production process based on adaptive design of experiments and bayesian optimization. Journal of Advanced Manufacturing and Processing 3, e10085. URL: https://aiche.onlinelibrary.wiley.com/doi/abs/10.1002/amp2.10085, doi:https://doi.org/10.1002/amp2.10085.

Kadar, J., Gackstatter, F., Ortner, F., Wagner, L., Willer, M., Preuster, P., Wasserscheid, P., Geißelbrecht, M., 2024. Boosting power density of hydrogen release from lohc systems by an inverted fixed-bed reactor design. International Journal of Hydrogen Energy 59, 1376–1387. URL: https://www.sciencedirect.com/science/article/pii/S0360319924005068, doi:https://doi.org/10.1016/j.ijhydene.2024.02.096.

Kazikova, A., Pluhacek, M., Senkerik, R., 2021. How does the number of objective function evaluations impact our understanding of metaheuristics behavior? IEEE Access 9, 44032–44048. doi:10.1109/ACCESS.2021.3066135.

Korberg, A., Brynolf, S., Grahn, M., Skov, I., 2021. Techno-economic assessment of advanced fuels and propulsion systems in future fossil-free ships. Renewable and Sustainable Energy Reviews 142, 110861. URL: https://www.sciencedirect.com/science/article/pii/S1364032121001556, doi:https://doi.org/10.1016/j.rser.2021.110861.

Laursen, R., Patel, H., Dowling, M., Sofiadi, D., Ji, C., Nelissen, D., Király, J., van der Veen, R., Pang, E., 2023. Potential of hydrogen as fuel for shipping. American Bureau of Shipping, European Maritime Safety Agency 571.

Martínez-Gomez, J., Peña-Lamas, J., Martín, M., Ponce-Ortega, J.M., 2017. A multi-objective optimization approach for the selection of working fluids of geothermal facilities: Economic, environmental and social aspects. Journal of Environmental Management 203, 962–972. URL: https://www.sciencedirect.com/science/article/pii/S0301479717306679, doi:https://doi.org/10.1016/j.jenvman.2017.07.001. environmental management as a pillar for sustainable development.

MEPC, R., 2023. 2023 imo strategy on reduction of ghg emissions from ships .

Morlet-Espinosa, J., Flores-Tlacuahuac, A., 2024. A bayesian optimization approach for data-driven mixed-integer nonlinear programming problems. AIChE Journal 70, e18448. URL: https://aiche.onlinelibrary.wiley.com/doi/abs/10.1002/aic.18448, doi:https://doi.org/10.1002/aic.18448.

Müller, K., Stark, K., Emel'yanenko, V.N., Varfolomeev, M.A., Zaitsau, D.H., Shoifet, E., Schick, C., Verevkin, S.P., Arlt, W., 2015. Liquid organic hydrogen carriers: Thermophysical and thermochemical studies of benzyl- and dibenzyl-toluene derivatives. Industrial & Engineering Chemistry Research 54, 7967–7976. doi:10.1021/acs.iecr.5b01840.

Nakayama, Y., Kaneko, H., 2023. Robust design of a dimethyl ether production process using process simulation and robust bayesian optimization. ACS Omega 8, 29161–29168. doi:10.1021/acsomega.3c02344.

Niermann, M., Beckendorff, A., Kaltschmitt, M., Bonhoff, K., 2019. Liquid organic hydrogen carrier (lohc) – assessment based on chemical and economic properties. International Journal of Hydrogen Energy 44, 6631–6654. URL: https://www.sciencedirect.com/science/article/pii/S0360319919303581, doi:https://doi.org/10.1016/j.ijhydene.2019.01.199.

Nocedal, J., Wright, S.J., 2006. Numerical optimization. Springer.

Ong, J.H., Teo, J., 2021. Systematic review and open challenges in hyper-heuristics usage on expensive optimization problems with limited number of evaluations, in: 2021 IEEE Symposium on Industrial Electronics & Applications (ISIEA), pp. 1–6. doi:10.1109/ISIEA51897.2021.9509993.

Paulson, J.A., Tsay, C., 2025. Bayesian optimization as a flexible and efficient design framework for sustainable process systems. Current Opinion in Green and Sustainable Chemistry 51, 100983. URL: https://www.sciencedirect.com/science/article/pii/S2452223624001044, doi:https://doi.org/10.1016/j.cogsc.2024.100983.

Peters, R., Deja, R., Engelbracht, M., Frank, M., Nguyen, V.N., Blum, L., Stolten, D., 2016. Efficiency analysis of a hydrogen-fueled solid oxide fuel cell system with anode off-gas recirculation. Journal of Power Sources 328, 105–113. URL: https://www.sciencedirect.com/science/article/pii/S0378775316310011, doi:https://doi.org/10.1016/j.jpowsour.2016.08.002.

Planas-Cuchi, E., Vílchez, J.A., Casal, J., 1999. Fire and explosion hazards during filling/emptying of tanks. Journal of Loss Prevention in the Process Industries 12, 479–483. URL: https://www.sciencedirect.com/science/article/pii/S0950423099000169, doi:https://doi.org/10.1016/S0950-4230(99)00016-9.

Preuster, P., Fang, Q., Peters, R., Deja, R., Nguyen, V.N., Blum, L., Stolten, D., Wasserscheid, P., 2018. Solid oxide fuel cell operating on liquid organic hydrogen carrier-based hydrogen – making full use of heat integration potentials. International Journal of Hydrogen Energy 43, 1758–1768. URL: https://www.sciencedirect.com/science/article/pii/S0360319917343719, doi:https://doi.org/10.1016/j.ijhydene.2017.11.054.

Prieto, C., Sánchez, A., Martín, M., 2023. A three-phase reactor assessment for the deployment of liquid organic hydrogen carriers (lohcs): dybenzyltoluene and indoles mixture systems as case studies. Energy Conversion and Management 294, 117548. URL: https://www.sciencedirect.com/science/article/pii/S0196890423008944, doi:https://doi.org/10.1016/j.enconman.2023.117548.

Prieto, C., Sánchez, A., Martín, M., 2025. A two-step methodology for the selection and process optimization of liquid organic hydrogen carriers (lohcs). International Journal of Hydrogen Energy 135, 69–85. URL: https://www.sciencedirect.com/science/article/pii/S0360319925020580, doi:https://doi.org/10.1016/j.ijhydene.2025.04.371.

Rao, N., Lele, A.K., Patwardhan, A.W., 2022. Optimization of liquid organic hydrogen carrier (lohc) dehydrogenation system. International Journal of Hydrogen Energy 47, 28530–28547. URL: https://www.sciencedirect.com/science/article/pii/S0360319922028324, doi:https://doi.org/10.1016/j.ijhydene.2022.06.197.

Reuß, M., Grube, T., Robinius, M., Preuster, P., Wasserscheid, P., Stolten, D., 2017. Seasonal storage and alternative carriers: A flexible hydrogen supply chain model. Applied Energy 200, 290–302. URL: https:

//www.sciencedirect.com/science/article/pii/S0306261917305457, doi:https://doi.org/10.1016/j.apenergy.2017.05.050.

Satterfield, C.N., 1975. Trickle-bed reactors. AIChE Journal 21, 209–228.

Shariff, A.M., Leong, C.T., Zaini, D., 2012. Using process stream index (psi) to assess inherent safety level during preliminary design stage. Safety Science 50, 1098–1103. URL: https://www.sciencedirect.com/science/article/pii/S0925753511003055, doi:https://doi.org/10.1016/j.ssci.2011.11.015. first International Symposium on Mine Safety Science and Engineering 2011.

Siemens Energy, 2021. Green shipping programme: Infrastructure for liquid organic hydrogen carrier (lohc). URL: https://greenshippingprogramme.com/pilot/infrastructure-for-liquid-organic-hydrogen-carrier-lohc/.

Sinnott, R., Towler, G., 2020. Chapter 12 - heat-transfer equipment, in: Sinnott, R., Towler, G. (Eds.), Chemical Engineering Design (Sixth Edition). sixth edition ed.. Butterworth-Heinemann. Chemical Engineering Series, pp. 773–927. URL: https://www.sciencedirect.com/science/article/pii/B9780081025994000126, doi:https://doi.org/10.1016/B978-0-08-102599-4.00012-6.

Szparaga, A., Stachnik, M., Czerwińska, E., Kocira, S., Dymkowska-Malesa, M., Jakubowski, M., 2019. Multi-objective optimization based on the utopian point method applied to a case study of osmotic dehydration of plums and its storage. Journal of Food Engineering 245, 104–111. URL: https://www.sciencedirect.com/science/article/pii/S0260877418304412, doi:https://doi.org/10.1016/j.jfoodeng.2018.10.014.

van de Berg, D., Savage, T., Petsagkourakis, P., Zhang, D., Shah, N., del Rio-Chanona, E.A., 2022. Data-driven optimization for process systems engineering applications. Chemical Engineering Science 248, 117135. URL: https://www.sciencedirect.com/science/article/pii/S0009250921007004, doi:https://doi.org/10.1016/j.ces.2021.117135.

Verhoolen, A., Geißelbrecht, M., Kadar, J., Preuster, P., Wasserscheid, P., Graichen, K., 2024. Bayesian optimization of operating points of a continuous perhydro-dibenzyltoluene dehydrogenation reactor. International Journal of Energy Research 2024, 5627453. URL: https://onlinelibrary.wiley.com/doi/abs/10.1155/2024/5627453, doi:https://doi.org/10.1155/2024/5627453.

Virtanen, P., Gommers, R., Oliphant, T.E., Haberland, M., Reddy, T., Cournapeau, D., Burovski, E., Peterson, P., Weckesser, W., Bright, J., van der Walt, S.J., Brett, M., Wilson, J., Millman, K.J., Mayorov, N., Nelson, A.R.J., Jones, E., Kern, R., Larson, E., Carey, C.J., Polat, İ., Feng, Y., Moore, E.W., VanderPlas, J., Laxalde, D., Perktold, J., Cimrman, R., Henriksen, I., Quintero, E.A., Harris, C.R., Archibald, A.M., Ribeiro, A.H., Pedregosa, F., van Mulbregt, P., SciPy 1.0 Contributors, 2020. SciPy 1.0: Fundamental Algorithms for Scientific Computing in Python. Nature Methods 17, 261–272. doi:10.1038/s41592-019-0686-2.

Ward, A., Pini, R., 2022. Efficient bayesian optimization of industrial-scale pressure-vacuum swing adsorption processes for co2 capture. Industrial & Engineering Chemistry Research 61, 13650–13668. doi:10.1021/acs.iecr.2c02313.

Willer, M., Preuster, P., Geißelbrecht, M., Wasserscheid, P., 2024a. Continuous dehydrogenation of perhydro benzyltoluene and perhydro dibenzyltoluene in a packed bed vertical tubular reactor – the role of lohc evaporation. International Journal of Hydrogen Energy 57, 1513–1523. URL: https://www.sciencedirect.com/science/article/pii/S0360319924000338, doi:https://doi.org/10.1016/j.ijhydene.2024.01.031.

Willer, M., Preuster, P., Malgaretti, P., Harting, J., Wasserscheid, P., 2024b. Heat transfer to a catalytic multiphase dehydrogenation reactor. International Journal of Hydrogen Energy 80, 1011–1020. URL: https://www.sciencedirect.com/science/article/pii/S0360319924027393, doi:https://doi.org/10.1016/j.ijhydene.2024.07.073.

Wu, Y., Walsh, A., Ganose, A.M., 2024. Race to the bottom: Bayesian optimisation for chemical problems. Digital Discovery 3, 1086–1100. URL: http://dx.doi.org/10.1039/D3DD00234A, doi:10.1039/D3DD00234A.

Zabetakis, M.G., 1964. Flammability characteristics of combustible gases and vapors. Technical Report. Bureau of Mines, Pittsburgh, PA (United States).

Zhang, Y., Apley, D.W., Chen, W., 2020. Bayesian optimization for materials design with mixed quantitative and qualitative variables. Scientific reports 10, 4924.

Zhao, Z., Kubal, J., Abraham, D., Ryan, E., 2025. Benchmarking optimization methods for materials research: Gradient descent and bayesian optimization for lithium-ion battery aging diagnostics. Journal of Power Sources 656, 238049. URL: https://www.sciencedirect.com/science/article/pii/S0378775325018853, doi:https://doi.org/10.1016/j.jpowsour.2025.238049.